Article

Immunity

Airway Memory CD4$^+$ T Cells Mediate Protective Immunity against Emerging Respiratory Coronaviruses

Highlights

- Intranasal but not subcutaneous vaccination protects mice from pathogenic human CoVs
- Protection is mediated by airway memory CD4$^+$ T cells
- IFN-γ produced by airway memory CD4$^+$ T cells is required for protection
- A conserved epitope in SARS-CoV and MERS-CoV induces cross-reactive T cell responses

Authors

Jincun Zhao, Jingxian Zhao, Ashutosh K. Mangalam, ..., Ralph S. Baric, Chella S. David, Stanley Perlman

Correspondence

zhaojincun@gird.cn (J.Z.), stanley-perlman@uiowa.edu (S.P.)

In Brief

Zoonotic CoVs have emerged twice in the past 10 years and have caused severe human respiratory disease. Using an alphavirus vaccine vector, Perlman and colleagues show that intranasal vaccination induces airway memory CD4$^+$ T cell responses that protect mice from lethal challenge and are cross-reactive to different CoVs.

Zhao et al., 2016, Immunity *44*, 1379–1391
June 21, 2016
http://dx.doi.org/10.1016/j.immuni.2016.05.006

CellPress

Immunity
Article

Airway Memory CD4$^+$ T Cells Mediate Protective Immunity against Emerging Respiratory Coronaviruses

Jincun Zhao,[1,2,6,*] Jingxian Zhao,[2,6] Ashutosh K. Mangalam,[3] Rudragouda Channappanavar,[2] Craig Fett,[2] David K. Meyerholz,[3] Sudhakar Agnihothram,[4,7] Ralph S. Baric,[4] Chella S. David,[5] and Stanley Perlman[2,*]
[1]State Key Laboratory of Respiratory Diseases, Guangzhou Institute of Respiratory Disease, The First Affiliated Hospital of Guangzhou Medical University, Guangzhou 510120, China
[2]Department of Microbiology
[3]Department of Pathology
University of Iowa, Iowa City, IA 52242, USA
[4]Department of Microbiology and Immunology and Department of Epidemiology, University of North Carolina, Chapel Hill, NC 27599, USA
[5]Department of Immunology, Mayo Clinic, Rochester, MI 55905, USA
[6]Co-first author
[7]Present address: National Center for Toxicological Research, Food and Drug Administration, Jefferson, AK 72079, USA
*Correspondence: zhaojincun@gird.cn (J.Z.), stanley-perlman@uiowa.edu (S.P.)
http://dx.doi.org/10.1016/j.immuni.2016.05.006

SUMMARY

Two zoonotic coronaviruses (CoVs)—SARS-CoV and MERS-CoV—have crossed species to cause severe human respiratory disease. Here, we showed that induction of airway memory CD4$^+$ T cells specific for a conserved epitope shared by SARS-CoV and MERS-CoV is a potential strategy for developing pan-coronavirus vaccines. Airway memory CD4$^+$ T cells differed phenotypically and functionally from lung-derived cells and were crucial for protection against both CoVs in mice. Protection was dependent on interferon-γ and required early induction of robust innate and virus-specific CD8$^+$ T cell responses. The conserved epitope was also recognized in SARS-CoV- and MERS-CoV-infected human leukocyte antigen DR2 and DR3 transgenic mice, indicating potential relevance in human populations. Additionally, this epitope was cross-protective between human and bat CoVs, the progenitors for many human CoVs. Vaccine strategies that induce airway memory CD4$^+$ T cells targeting conserved epitopes might have broad applicability in the context of new CoVs and other respiratory virus outbreaks.

INTRODUCTION

QA The coronavirus (CoV) Middle East respiratory syndrome (MERS)-CoV is a newly emerging pathogen that continues to cause outbreaks in the Arabian peninsula and in travelers from this region. As of April 24, 2016, a total of 1,724 cases with 623 deaths (36.1% mortality) were reported to the World Health Organization. Another human pathogenic CoV, severe acute respiratory syndrome (SARS-CoV), caused more than 8,000 human infections in 2002–2003, with a 10% mortality rate (Peiris et al., 2004). The presence of SARS-like CoV and other CoVs in zoonotic populations as well as the ongoing MERS epidemic make it likely that additional CoV outbreaks will emerge (Ge et al., 2013). These possibilities indicate the need for development of vaccines that would be effective against many strains of CoVs.

Most CoV vaccines presently under development target the most variable part of the spike glycoprotein and induce antibody responses only against the virus present in the vaccine. However, even that virus can undergo antibody escape (Ma et al., 2014; Sui et al., 2014). Antibody responses in patients previously infected with respiratory viruses, including SARS-CoV and influenza A virus (IAV), tend to be short lived (Channappanavar et al., 2014; Wilkinson et al., 2012). On the other hand, T cell responses often target highly conserved internal proteins and are long lived. SARS-CoV-specific memory T cells but not B cells could be detected 6 years after infection in SARS survivors (Tang et al., 2011). Further, IAV-specific memory CD4$^+$ T cell numbers correlated with protection against the influenza strain H1N1 infection during the 2009 epidemic (Wilkinson et al., 2012).

Memory CD4$^+$ T cells are more numerous at sites of infection than CD8$^+$ T cells (Turner and Farber, 2014) and have multiple roles in initiating and propagating the immune response (Swain et al., 2012). However, much less is known about how these cells provide protection and whether localization of these cells at specific sites within tissue is critical (Turner and Farber, 2014). In the respiratory tract, memory CD4$^+$ T cells include cells in the airway and parenchyma and cells adhering to the pulmonary vasculature. Airway memory CD4$^+$ T cells are the first cells to encounter viral antigen during respiratory infections, suggesting a key role in protection. However, it is not clear whether airway and parenchymal cells differentially mediate protection during respiratory infections.

Here, we show that intranasal vaccination with Venezuelan equine encephalitis replicons (VRP) encoding a SARS-CoV CD4$^+$ T cell epitope induces airway CoV-specific memory CD4$^+$ T cells that efficiently protected mice against lethal disease through rapid local IFN-γ production. The epitope used was conserved in MERS-CoV, was presented by human leukocyte

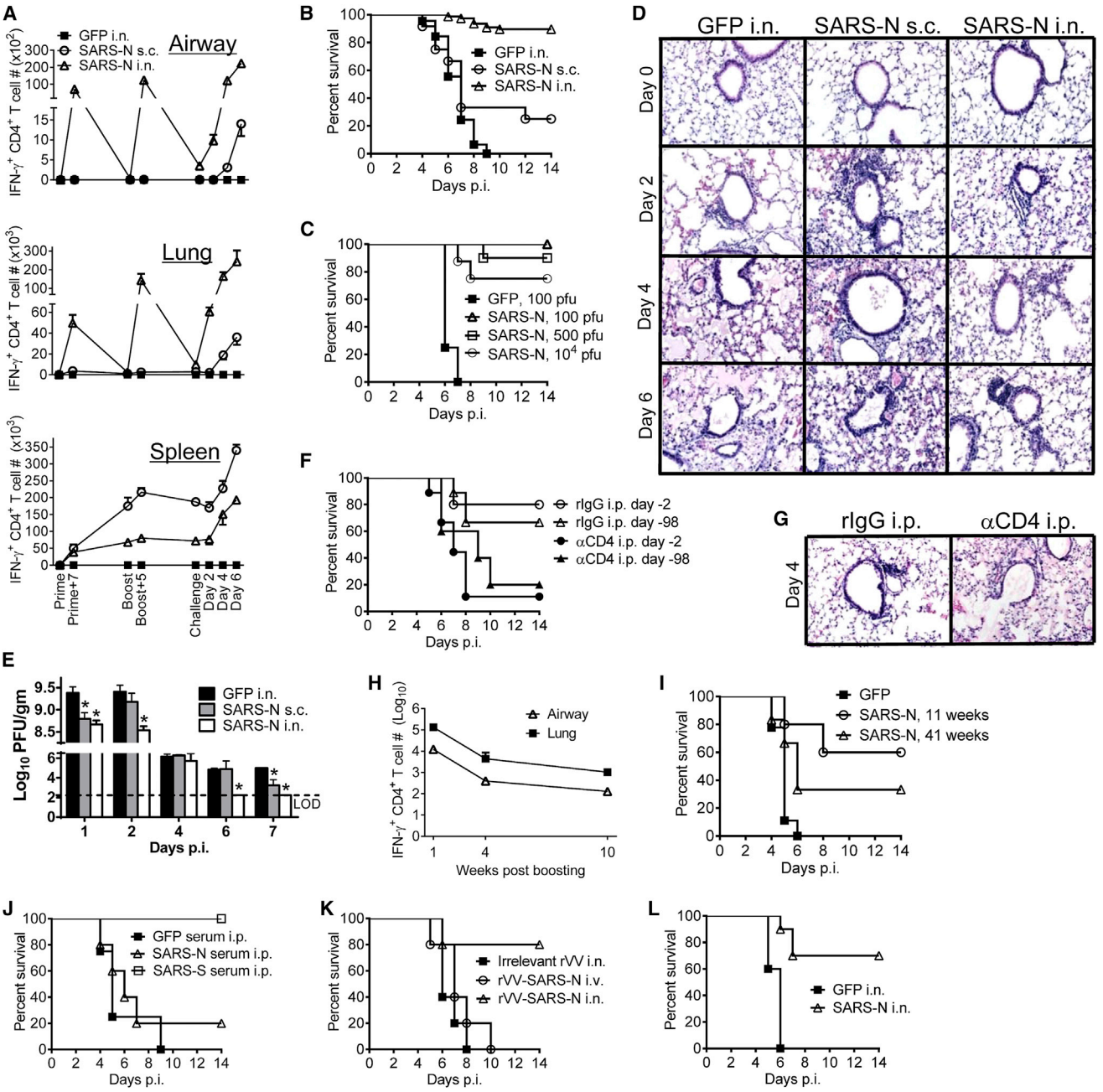

Figure 1. Intranasal Vaccination with VRP-SARS-N Results in CD4⁺ T-Cell-Dependent Protection against Lethal SARS-CoV Infection

6-week-old BALB/c mice were vaccinated with VRP-GFP or VRP-SARS-N subcutaneously (s.c.) in the footpad or intranasally (i.n.) and boosted 6–7 weeks later.

(A) Vaccinated mice were infected with SARS-CoV at the indicated times. Cells from airway, lung, and spleen were stimulated with SARS-N353 peptide. Numbers of IFN-γ^+CD4$^+$ T cells are shown.

(B) Survival after infection with 500 PFU SARS-CoV 4–6 weeks after boosting. n = 12, SARS-N s.c.; n = 77, SARS-N i.n.; n = 45, GFP i.n.

(C) Intranasally vaccinated mice were infected with various doses of SARS-CoV. n = 4, GFP 100 PFU; n = 4, SARS-N 100 PFU; n = 10, SARS-N 500 PFU; n = 8, SARS-N 10^4 PFU.

(D) Lungs were removed at the indicated times p.i., and sections were stained with hematoxylin and eosin.

(E) To obtain virus titers, lungs were homogenized at the indicated time points and titered on Vero E6 cells. Titers are expressed as PFU/g tissue. n = 3 mice/group/time point. *$p < 0.05$. Data are representative of two independent experiments.

(F) VRP-SARS-N-vaccinated mice were treated intraperitoneally (i.p.) with 1 mg anti-CD4 antibody (clone GK1.5) or rat IgG (rIgG) at day −2 and day 0 p.i. (day 2); some mice were rested for 98 days before SARS-CoV infection (day 98). n = 5, rIgG i.p. day −2; n = 9, αCD4 i.p. day −2; n = 9, rIgG i.p. day −98; n = 5, αCD4 i.p. day −98.

(G) Lungs were removed from VRP-SARS-N-vaccinated and antibody i.p.-treated mice at day 4 p.i. Sections were stained with hematoxylin and eosin.

(H) Numbers of IFN-γ^+CD4$^+$ T cells at several times after boosting are shown.

(legend continued on next page)

antigen (HLA) DR2 and DR3 molecules, and mediated cross protection between SARS-CoV and MERS-CoV and related bat CoV. These results indicate that induction of airway memory $CD4^+$ T cells should be considered as a component of any universal human coronavirus vaccine and potentially, those targeting other respiratory viruses.

RESULTS

Intranasal Vaccination with VRP-SARS-N Results in $CD4^+$ T Cell-Dependent Protection against SARS-CoV

Previously, we identified a dominant $CD4^+$ T cell epitope in the nucleocapsid (N) protein of SARS-CoV (N353) recognized in BALB/c ($H\text{-}2^d$) mice; no $CD8^+$ T cell epitopes are present in this protein (Zhao et al., 2010). This region of N is also targeted by $CD4^+$ T cells from SARS convalescent patients (Oh et al., 2011; Peng et al., 2006). We initially evaluated whether intranasal (i.n.) immunization, which generates local $CD4^+$ T cell responses, or footpad vaccination, which generates a systemic T cell response, resulted in differences in protection against challenge with mouse-adapted SARS-CoV (Roberts et al., 2007). For this purpose, we vaccinated BALB/c mice twice at 6–7 week intervals with VRP-SARS-N or a control VRP expressing green fluorescent protein (VRP-GFP) i.n. or subcutaneously (s.c.) prior to challenge. VRPs are non-replicating vaccine vectors that preferentially infect human and mouse dendritic cells and serve as self-adjuvants (Moran et al., 2005; Tonkin et al., 2012). Only i.n. inoculation with VRP-SARS-N induced an N-specific $CD4^+$ T cell response in the lungs and airways, which was increased by i.n. VRP-SARS-N boosting (Figure 1A). In contrast, s.c. inoculation resulted in a $CD4^+$ T cell response primarily in the spleen with virtually no N-specific T cells identified in the lungs or airway. Subcutaneous boosting increased the numbers of virus-specific cells in the spleen but not in respiratory tissue. As expected, VRP-SARS-N administration resulted in accumulation of N-expressing DCs and, consequently, more N-specific $CD4^+$ T cells in the draining mediastinal lymph nodes (MLNs; i.n. immunization) and popliteal lymph nodes (PLNs; s.c. immunization) (Figure S1). Protection from lethal disease was nearly complete after i.n. but not s.c. administration of VRP-SARS-N, demonstrating the importance of the route of vaccination (Figure 1B). Protection was observed against challenge with doses ranging from 100 to 10,000 PFUs of SARS-CoV (Figure 1C). By days 4–6 after challenge, SARS-CoV-infected VRP-GFP-immunized mice develop severe edema with a relative paucity of infiltrating cells whereas intranasal VRP-SARS-N-immunized mice displayed prominent peribronchiolar and perivascular infiltration and minimal amounts of edema in the lungs. Subcutaneous immunization with VRP-SARS-N did not protect against edema formation (Figure 1D). Consistent with these results, intranasal VRP-SARS-N immunization enhanced the kinetics of virus clearance (Figure 1E). Next we assessed the role of memory $CD4^+$ T cells in protection by depleting them systemically 2 days prior to challenge. This abrogated protection (Figures 1F and S2A), indicating that memory $CD4^+$ T cells might be important for protection.

In a subsequent set of experiments, to confirm the importance of memory $CD4^+$ T cells, vaccinated mice were treated with $CD4^+$ T-cell-depleting antibody 98 days prior to challenge to allow $CD4^+$ T cell recovery (Figure S2B). These mice were not protected against SARS-CoV challenge (Figure 1F) and developed histological changes similar to those observed in VRP-GFP-immunized mice (Figure 1G). N-specific $CD4^+$ T cell numbers gradually decreased after vaccination (Figure 1H) but still mediated partial protection after challenge at 41 weeks after boosting (Figure 1I). $CD4^+$ T cells provide helper function for antibody production, but unlike sera from VRP-SARS-S, which induced neutralizing antibody, sera from VRP-SARS-N-immunized mice were not protective upon transfer to naive mice prior to challenge (Figure 1J). Protection was also observed in mice immunized with another vaccine, recombinant vaccinia virus expressing the N protein (rVV-SARS-N) (Figure 1K). Because the $CD4^+$ T cell response was more robust in VRP- compared to rVV-immunized mice (data not shown), we used VRP-SARS-N for the remainder of the subsequent experiments. 12-month-old mice are very susceptible to SARS-CoV (Zhao et al., 2011); however, VRP-SARS-N vaccination at 12 months and analysis at 15 months of age resulted in protection against challenge, demonstrating efficacy even in this highly vulnerable population (Figure 1L). Together, these results indicate that intranasal but not subcutaneous immunization induced a protective $CD4^+$ T cell immune response.

Airway-Derived N-Specific $CD4^+$ T Cells Are Superior Effector Cells

Although these results demonstrated that SARS-CoV N-specific memory $CD4^+$ T cells in the respiratory tract were protective, they did not distinguish between cells localized in the airway, parenchyma, and vasculature. To discriminate between cells localized to the airway versus those in the parenchyma and vasculature, we used a modification of a previously described method (Anderson et al., 2012) to simultaneously label cells by i.v. and i.n. administration of CD90.2 and CD45 antibodies, respectively, 5–7 weeks after boosting. Consistent with $CD8^+$ T cell studies, a large proportion of $CD4^+$ T cells in the respiratory tract were localized in the vasculature (Figure 2A; Anderson et al., 2012). Additionally, the vast majority of cells in the airway were not labeled by i.v. antibody administration, indicating their anatomic compartmentalization (Figure 2A). N353-specific $CD4^+$ T cells comprised a higher percentage of cells in the airway compared to the parenchymal or vascular populations, although the greatest number of SARS-CoV-specific cells were present in the

(I) Survival after infection with 100 PFU SARS-CoV at 11 and 41 weeks after boosting. n = 9, GFP; n = 5, SARS-N 11 weeks; n = 6, SARS-N 41 weeks.
(J) 300 μL of immune serum were transferred into VRP-GFP-vaccinated mice 1 day before infection. n = 4, GFP serum i.p.; n = 5, SARS-N serum i.p.; n = 5, SARS-S serum i.p.
(K) Mice were vaccinated with rVV-SARS-N or irrelevant rVV intravenously (i.v.) or i.n. and boosted 6–7 weeks later. Mice were infected with SARS-CoV 4–6 weeks after boosting. n = 5/group.
(L) 15-month-old VRP-SARS-N-vaccinated mice were infected with 100 PFU SARS-CoV. n = 5, GFP i.n.; n = 10, SARS-N i.n.
Error bars in (A) and (E) represent SEM. See also Figures S1, S2, and S6.

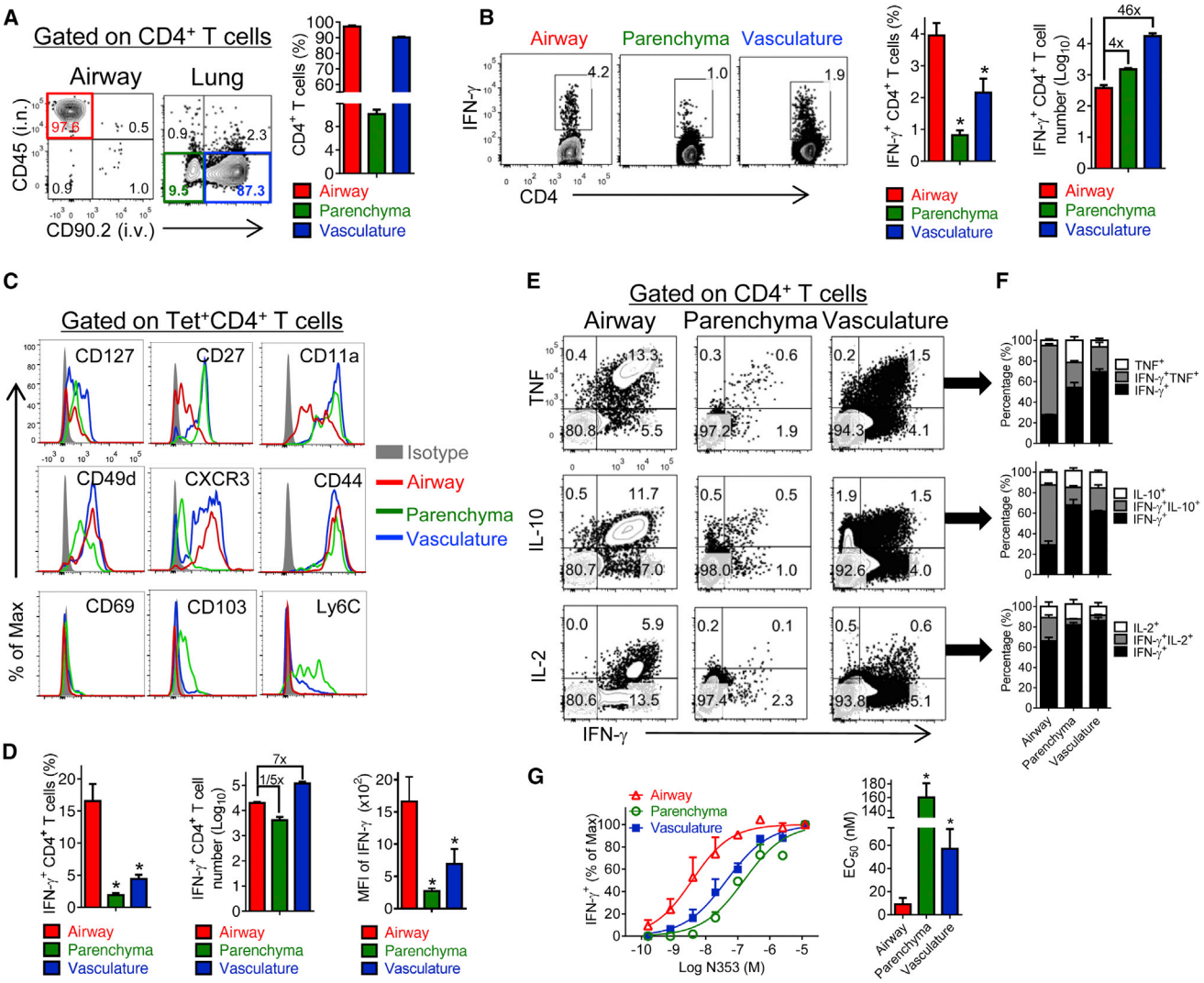

Figure 2. Airway-Derived N-Specific CD4⁺ T Cells Are Superior Effector Cells

(A) To localize memory CD4⁺ T cells in the respiratory tract at 5–7 weeks after boosting, 0.25 μg of fluorochrome-conjugated CD45 and 0.5 μg of fluorochrome-conjugated CD90.2 antibody were injected i.n. and i.v., respectively, as described in the Experimental Procedures.

(B) CD4⁺ T cells from airway, parenchyma, and vasculature were stimulated with SARS-CoV N353 peptide. Data are representative of five independent experiments.

(C) Cells from vaccinated mice were stained with SARS-N353 tetramer and phenotypic markers at 5–7 weeks after boosting after simultaneous i.n./i.v. labeling. Data are representative of two independent experiments.

(D–G) Vaccinated mice were infected with SARS-CoV at the indicated times. Cells were stimulated with SARS-N353 peptide. Frequency, numbers, and mean fluorescence intensity (MFI) of IFN-γ expression (D) of IFN-γ⁺CD4⁺ T cells or cells expressing IFN-γ and TNF, IL-10, or IL-2 (E and F) are shown. *$p < 0.05$. Data are representative of three independent experiments.

(G) Functional avidity of N353-specific CD4⁺ T cells (left) and the amount of peptide required for half-maximum response (EC_{50}) are shown (right). *$p < 0.05$. Data are representative of four independent experiments.

Error bars in (B), (D), (F), and (G) represent SEM. See also Figures S3 and S5.

vasculature (Figure 2B). Airway, parenchymal, and vascular N353 memory CD4⁺ T cells differed phenotypically. Surface molecules associated with memory (CD127 and CD27) and trafficking (CD11a) were expressed at lower levels on airway cells compared to cells in the parenchyma or vasculature. Unlike memory CD8⁺ T cells localized in tissues, airway memory CD4⁺ T cells did not express CD69, CD103, and Ly6C although CD69 was expressed after priming (data not shown). Parenchymal cells expressed CD103 and Ly6C (Figure 2C; Mueller et al., 2013).

Next, we examined whether cells in the airway, which first encounter viral antigen, were critical for mediating protection after challenge. After SARS-CoV challenge, the percentage of N-specific CD4⁺ T cells was much higher in the airway and the number of N353 CD4⁺ T cells at this site increased substantially compared to those in the parenchyma and vasculature

(Figure 2D). Also, airway N353 CD4$^+$ T cells expressed IFN-γ at higher levels on a per cell basis compared to the parenchyma and vasculature (Figures 2D and 2E). Airway cells had superior effector function, indicated by the ability to express more than one cytokine (TNF, IL-10, IL-2) (Figure 2E). In addition, these multi-functional CD4$^+$ T cells were present at a higher frequency in the airway compared to parenchyma and vasculature (Figure 2F) and exhibited greater functional avidity (Figure 2G). To determine whether the increase in N353 CD4$^+$ T cells reflected local proliferation or recruitment, infected mice were treated with FTY720 to prevent T cell egress from lymphoid tissue and then treated at day 4 p.i. with BrdU for 4 hr (Figure S3). FTY720 treatment decreased the numbers of N-specific CD4$^+$ T cells in the respiratory tract and the remaining cells showed evidence of BrdU incorporation, indicating roles for both recruitment and proliferation in augmentation of N353 CD4$^+$ T cells. These results indicate that memory CD4$^+$ T cells in the airway were phenotypically and functionally different from those in the parenchyma and vasculature, were maintained by both local proliferation and recruitment, and were potentially most important for protection.

N-Specific Airway Memory CD4$^+$ T Cells Mediate Protection by Local Expression of IFN-γ

To address more explicitly the role of airway cells in protection, we depleted CD4$^+$ T cells in the airways, but not the parenchyma or vasculature, by i.n. administration of 10 μg anti-CD4$^+$ T cell antibody prior to challenge (Figure 3A). Previous reports indicated a key role for resident memory T (Trm) cells (T cells that are present at sites of prior infection without recirculation) in protection against pathogen challenge (Masopust and Picker, 2012; Mueller et al., 2013; Turner and Farber, 2014) and CD4$^+$ Trm cells have been identified in the context of influenza A virus infection (Teijaro et al., 2011). However, these airway N353 cells did not fit the classic definition of resident memory T cells because they were replenished by 4 weeks after depletion (Figure 3B), similar to airway memory IAV-specific CD8$^+$ T cells (Slütter et al., 2013). Depletion decreased survival to approximately 35%, demonstrating the key role that airway memory CD4$^+$ T cells have in protection (Figure 3C). To probe the mechanism of action of these cells, we initially focused on type I interferon (IFN-I) expression because IFN-I orchestrates a protective response at early times p.i. IFN-α, IFN-β, and IFN-λ were not upregulated after VRP-SARS-N immunization. In contrast, higher IFN-γ mRNA levels were detected in the lungs of VRP-SARS-N-immunized mice by day 1 p.i. (Figures 3D and 3E). This cytokine was largely produced by airway CD4$^+$ T cells since local and systemic depletion of these cells was equally efficient in reducing IFN-γ expression in the lung (Figure 3E). Expression of other cytokines, such as TNF, IL-1β, IL-6, and IL-12, was not upregulated by prior VRP-SARS-N vaccination (Figure S4A). IFN-γ expression by airway CD4$^+$ T cells was confirmed using an in vivo cytokine expression assay, in which mice were treated with Brefeldin A (BFA) for 6 hr prior to direct ex vivo analysis without additional stimulation (Figure 3F; Hufford et al., 2011). Expression of IFN-γ by CD4$^+$ T cells resulted in the upregulation of several IFN-related genes in SARS-CoV-challenged, VRP-SARS-N-vaccinated mice, including STAT-1, PKR, and OAS-1, which are important for CoV clearance (Figure S4B; Frieman et al., 2010; Wang et al., 2009; Zhao et al., 2012). Neutralization of IFN-γ in the airway by i.n. administration prior to infection and every 2 days thereafter abrogated upregulation of these genes (Figure 3G).

Airway IFN-γ neutralization resulted in increased mortality (Figure 3H) and also in an increase in pathological changes (i.e., edema, alveolar destruction) in the lungs (Figure 3I). Both airway CD4$^+$ T cells and IFN-γ were required for maximal kinetics of virus clearance (Figure 3J), emphasizing the key role that these cells and cytokine played in protection, which was confirmed by demonstrating that airway administration of IFN-γ (but not TNF) resulted in 100% survival after SARS-CoV challenge (Figure 3K). Collectively, these results indicate that airway memory CD4$^+$ T cells were replenished from the lungs or periphery and that their protective function was largely mediated by IFN-γ.

Airway CD4$^+$ T-Cell-Derived IFN-γ Is Required for Optimal Respiratory Dendritic Cell Migration to MLNs

Although airway memory CD4$^+$ T cells and IFN-γ activated the innate immune response, virus clearance was also accelerated at late times p.i. (Figures 1E and 3J). This suggested that these cells had an additional role in enhancing the adaptive immune response, most likely the virus-specific CD8$^+$ T cell response, critical for SARS-CoV clearance (Channappanavar et al., 2014; Zhao et al., 2010). To generate robust CD8$^+$ T cell responses, respiratory dendritic cells (rDCs) must migrate to MLNs and prime naive CD8$^+$ T cells (Zhao et al., 2011). We next assessed whether airway memory CD4$^+$ T cells participated in these processes. In a role not previously reported, IFN-γ, largely expressed by these airway CD4$^+$ T cells, was critical for optimal rDC migration, as measured by increased frequency and number of lung-derived carboxyfluorescein succinimidyl ester (CFSE)-labeled rDCs in the MLN compared to VRP-GFP-immunized mice (Figure 4A). Administration of anti-CD4 or anti-IFN-γ antibody i.n. significantly reduced rDC migration to the MLNs, accompanied by decreased accumulation of total lymph node cells (Figure 4B). These rDCs in MLNs were mature and optimized for antigen presentation as shown by expression of co-stimulatory molecules such as CD40, CD80, and CD86. rDC migration to the MLN requires CCR7 expression and CCR7 was also upregulated on migratory rDCs in the MLNs (Figure 4C). IFN-γ augmented CCR7 expression since i.n. IFN-γ treatment resulted in a 10-fold increase in the frequency of lung CCR7$^+$ rDCs (Figure 4D). Together, these results established that airway memory CD4$^+$ T cells and IFN-γ secreted by these cells, in addition to activating the innate immune response, enhanced rDC migration to the MLN.

Airway CD4$^+$ T-Cell-Derived IFN-γ Promotes CXCR3-Dependent CD8$^+$ T Cell Mobilization to Infected Lung

SARS-CoV challenge of VRP-SARS-N-immunized mice resulted in an increase in frequency and numbers of lung CD8$^+$ T cells that recognized epitope S366 (the dominant epitope in BALB/c mice) when compared to VRP-GFP-immunized mice (Figure 5A). These CD8$^+$ T cells were functional, as shown by upregulation of granzyme B and CD107 (Figure 5B). We confirmed that these cells were cytotoxic in vivo by showing that i.n.-delivered peptide S366-coated target cells were specifically lysed in the lungs of immunized but not control mice (Figure 5C). Depletion of CD8$^+$

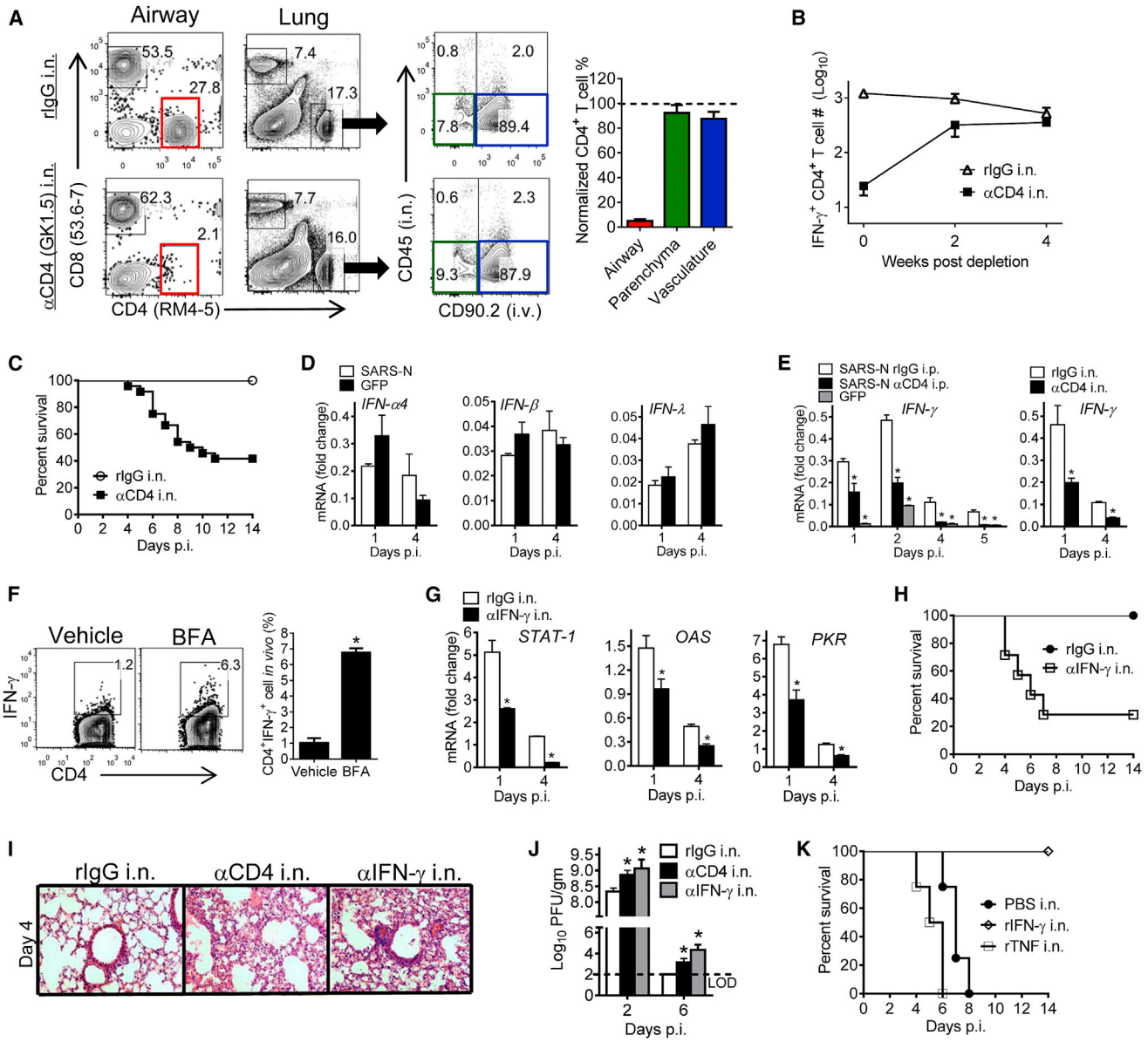

Figure 3. N-Specific Airway Memory CD4⁺ T Cells Mediate Protection by Local Expression of IFN-γ

(A and B) For local depletion of CD4⁺ T cells from the airway, mice were treated with 10 μg anti-CD4 antibody (clone GK1.5) i.n. in 75 μL PBS at day −1.

(A) Mice were simultaneously i.n. and i.v. labeled. BALF and lungs were harvested 2 days after depletion. Control mice received equivalent doses of rIgG in each experiment. Depletion efficiency was calculated.

(B) N353 CD4⁺ T cell numbers were monitored after depletion. n = 3 mice/group/time point. Data are representative of 2–4 independent experiments.

(C) Airway CD4⁺ T cells were depleted from VRP-SARS-N-vaccinated mice with anti-CD4 antibody or rIgG i.n. 1 day prior to SARS-CoV challenge. n = 5, rIgG i.n.; n = 24, αCD4 i.n.

(D) IFN mRNA levels in the lungs were measured at the indicated time points. n = 3–4 mice/group/time point. *$p < 0.05$. Data are representative of two independent experiments.

(E) CD4⁺ T cells were depleted from VRP-SARS-N-vaccinated mice prior to SARS-CoV infection by i.n. or i.p. administration of anti-CD4 antibody. IFN-γ RNA levels in the lungs were measured at the indicated time points. n = 3–6 mice/group/time point. *$p < 0.05$. Data are representative of two independent experiments.

(F) For in vivo ICS, VRP-SARS-N-vaccinated mice were treated i.n. with BFA or vehicle at day 4 p.i. After 6 hr, airway CD4⁺ T cells were analyzed for IFN-γ expression. Frequency of IFN-γ⁺CD4⁺ T cells is shown. *$p < 0.05$. Data are representative of two independent experiments.

(G) VRP-SARS-N-vaccinated mice were treated with 10 μg IFN-γ neutralizing antibody (clone XMG1.2) or rIgG i.n. at day −2 and every 2 days thereafter. Lungs were harvested at indicated time points and interferon-related gene RNA levels in the lungs were measured. n = 3–6 mice/group/time point. *$p < 0.05$. Data are representative of two independent experiments.

(H) VRP-SARS-N-vaccinated mice were treated with anti-IFN-γ antibody i.n. Control mice received equivalent doses of rIgG in each experiment. n = 5, rIgG; n = 9, αIFN-γ i.p.; n = 7, αIFN-γ i.n.

(I) Lungs were removed from VRP-SARS-N-vaccinated and antibody i.n.-treated mice at day 4 p.i. Sections were stained with hematoxylin and eosin.

(legend continued on next page)

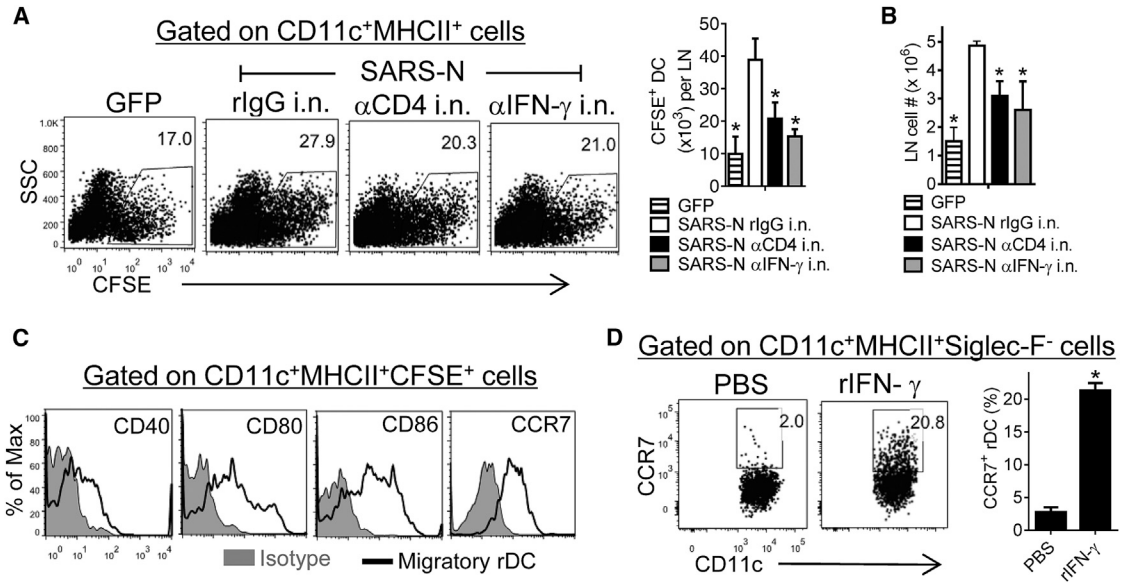

Figure 4. Airway CD4$^+$ T-Cell-Derived IFN-γ Is Required for Optimal rDC Migration to the MLNs

(A and B) To determine rDC migration from the lung to MLN, vaccinated mice were treated with anti-CD4 antibody, IFN-γ neutralizing antibody, or rIgG i.n. CFSE was then administered i.n. 6 hr before SARS-CoV infection. The percentage of CFSE$^+$ cells within the CD11c$^+$MHCII$^+$ DC population (A, left), total CFSE$^+$ DC numbers per LN (A, right), and total LN cell numbers (B) at 18 hr p.i. are shown. *$p < 0.05$. Data are representative of four independent experiments.

(C) CD40, CD80, CD86, and CCR7 expression on CFSE$^+$ rDCs in the MLN at 18 hr p.i. Isotype control is shaded.

(D) Naive mice were treated with 200 ng rIFN-γ i.n. for 12 hr. The frequency of CCR7$^+$ rDCs in lungs is shown. Data are representative of two independent experiments.

Error bars in (A), (B), and (D) represent SEM.

T cells prior to challenge resulted in decreased survival (Figures 5D and S2A) and delayed virus clearance at late times after infection (Figure 5E).

To assess the role of airway memory CD4$^+$ T cells in this enhanced CD8$^+$ T cell response, we depleted airway CD4$^+$ T cells or IFN-γ using antibodies and observed a decreased frequency and number of virus-specific CD8$^+$ T cells in the lungs (Figure 5F). Accumulation of cells in the lung requires T cell migration to this site, a process that is chemokine dependent. Virus-specific CD8$^+$ T cells expressed chemokine receptor CXCR3 but not CCR4 and CCR5 (Figure 5G), suggesting that effector CD8$^+$ T cell entry into the infected lung was dependent upon the CXCR3 pathway. In support of this, CXCR3 ligands CXCL9, CXCL10, and CXCL11 were expressed in the infected lungs in an airway CD4$^+$ T-cell- and IFN-γ-dependent manner (Figures 5H and S4C). We directly confirmed the importance of CXCR3 in CD8$^+$ T cell accumulation in the lungs by systemic blockade of CXCR3 at days 3 and 5 p.i. This treatment decreased the frequency and numbers of epitope S366-specific CD8$^+$ T cells in the lungs. Together these results showed that airway memory CD4$^+$ T cells orchestrated both rDC migration to the MLNs and virus-specific CD8$^+$ T cell trafficking to the lungs, enhancing clinical outcomes.

IL-10 Produced by Airway CD4$^+$ T Cells Is Required for Optimal Protection

T-cell-derived IL-10 is important for reducing immunopathology in infected mice (Sun et al., 2009; Trandem et al., 2011). However, IL-10 is not produced by T cells in SARS-CoV-infected mice (Zhao et al., 2010), which might contribute to more severe disease. In contrast, i.n. VRP-SARS-N vaccination induced IL-10 expression by SARS-N353-specific CD4$^+$ T cells in the lung after direct ex vivo (Figures 2E and 2F) or in vivo (Figures S5A–S5C) stimulation. IL-10 expression in the lungs was partly CD4$^+$ T cell and IFN-γ mediated (Figures S5A and S5B). IL-10 contributed to improved outcomes in VRP-SARS-N-immunized mice because IL-10 receptor blockade decreased survival (Figure S5D), without affecting the kinetics of virus clearance (Figure S5E). Thus, airway memory CD4$^+$ T cells expression of both pro-inflammatory (IFN-γ) and anti-inflammatory molecules was required for optimal protection.

VRP-SARS-N Immunization Does Not Result in Increased Eosinophil Infiltration into the Lungs

Previous studies of alum-adjuvanted killed SARS-CoV vaccines sometimes described eosinophilic infiltration into the lungs after challenge, suggestive of immunopathological disease (Bolles

(J) To obtain virus titers, mice were treated with antibody i.n. and sacrificed at the indicated time points. Titers are expressed as PFU/g tissue. n = 3 mice/group/time point. *$p < 0.05$. Data are representative of two independent experiments.

(K) Naive mice were treated with 200 ng rTNF or rIFN-γ 12 hr before SARS-CoV infection. n = 4, PBS i.n.; n = 5, rIFN-γ i.n.; n = 4, rTNF i.n.

Error bars in (A), (B), (D)–(G), and (J) represent SEM. See also Figure S4.

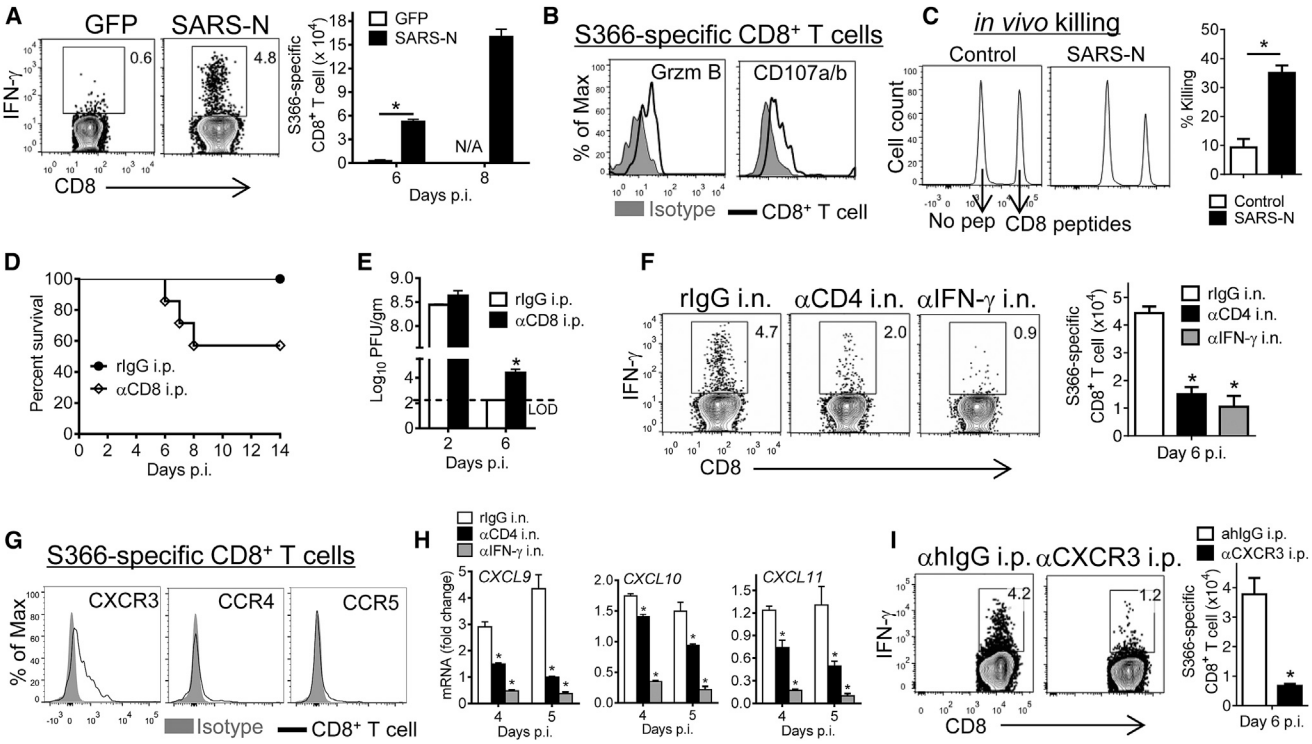

Figure 5. Airway CD4$^+$ T-Cell-Derived IFN-γ Promotes CXCR3-Dependent Mobilization of Virus-Specific CD8$^+$ T Cells to the Infected Lung

(A and B) Vaccinated mice were infected with SARS-CoV. At day 6 and 8 p.i., cells from lungs were stimulated with SARS-S366 peptide for IFN-γ (A) and granzyme B or CD107a/b expression (B).

(C) In vivo cytotoxicity assays in the lungs were performed on day 6 p.i. using SARS-CoV CD8$^+$ T cell peptide S366 as described in the Experimental Procedures. *$p < 0.05$. Data are representative of three independent experiments.

(D and E) For systemic depletion of CD8$^+$ T cells, VRP-SARS-N-vaccinated mice were injected i.p. with anti-CD8 or control antibody at day −2 and day 0 p.i. Mice were then infected with SARS-CoV and monitored for survival (D) (n = 5, rIgG i.p.; n = 7, αCD8 i.p.) or virus titers (E) (n = 3 mice/group/time point. *$p < 0.05$). Data are representative of two independent experiments.

(F) SARS-CoV S366-specific IFN-γ$^+$CD8$^+$ T cell frequency and numbers in the lungs of VRP-SARS-N-vaccinated and antibody i.n.-treated mice at day 6 p.i.

(G) Chemokine receptor expression on SARS-CoV S366-specific CD8$^+$ T cells at day 6 p.i.

(H) VRP-SARS-N-vaccinated mice were treated with anti-CD4 antibody or IFN-γ neutralizing antibody i.n. and infected with SARS-CoV. Lungs were assayed for chemokine RNA levels. n = 4–6 mice/group/time point. *$p < 0.05$. Data are representative of two independent experiments.

(I) SARS-CoV-challenged, VRP-SARS-N-vaccinated mice were treated with CXCR3 blocking antibody (clone CXCR3-173) i.p. at day 3 and 5 p.i. Lung cells were stimulated with SARS-S366 peptide at day 6 p.i.

Error bars in (A), (C), (E), (F), (H), and (I) represent SEM. See also Figures S2 and S4.

et al., 2011; Iwata-Yoshikawa et al., 2014). However, we could find no evidence of an eosinophilic infiltration into the lungs of either young or aged mice after i.n. or s.c. VRP-SARS-N immunization and challenge, when compared to mice vaccinated with a control VRP (Figures 1D and S6).

MERS-CoV N350 CD4$^+$ T Cell Epitope Elicits a Protective Response in BALB/c and HLA Transgenic Mice

Having established that airway memory CD4$^+$ T cells mediated protection against SARS-CoV challenge, we next assessed whether this approach was broadly applicable to other CoV infections, including MERS-CoV. First, we examined N proteins from several alpha and beta coronaviruses for a SARS-N353 epitope-like sequence. Epitope SARS-N353 was present in all SARS-like CoVs isolated from civet cats, Chinese ferret badgers, and bats. Bats are the reservoir for SARS-CoV and civet cats and Chinese ferret badgers served as intermediate hosts during the 2002–2003 pandemic (Chinese SARS Molecular Epidemiology Consortium, 2004; Ge et al., 2013; Li et al., 2005). In addition, similar sequences were detected in MERS-CoV and bat CoV HKU4, HKU5, and HKU9 as well as more distantly related alpha coronaviruses (Figure 6A). To determine whether MERS-N350 was recognized in infected mice, we challenged mice expressing the virus receptor, hDPP4 (human dipeptidyl peptidase 4) (Zhao et al., 2014) with MERS-CoV. MERS-N350-specific CD4$^+$ T cells were detected in infected BALB/c mice (Figure 6B). Next, mice were immunized with VRP-MERS-N, resulting in a robust airway CD4$^+$ T cell response that could be boosted by a second VRP-MERS-N immunization (Figure 6C). Consistent with results obtained after VRP-SARS N vaccination, these cells exhibited superior effector function, were multifunctional (Figure S7), and accelerated virus clearance upon challenge (Figure 6D). MERS-CoV N, unlike SARS-CoV N protein, encodes a weak CD8$^+$ T cell epitope in BALB/c mice (N214, LYLDLLNRL) (Zhao et al., 2014), which might have contributed to accelerated virus clearance. However, the contribution made by these cells

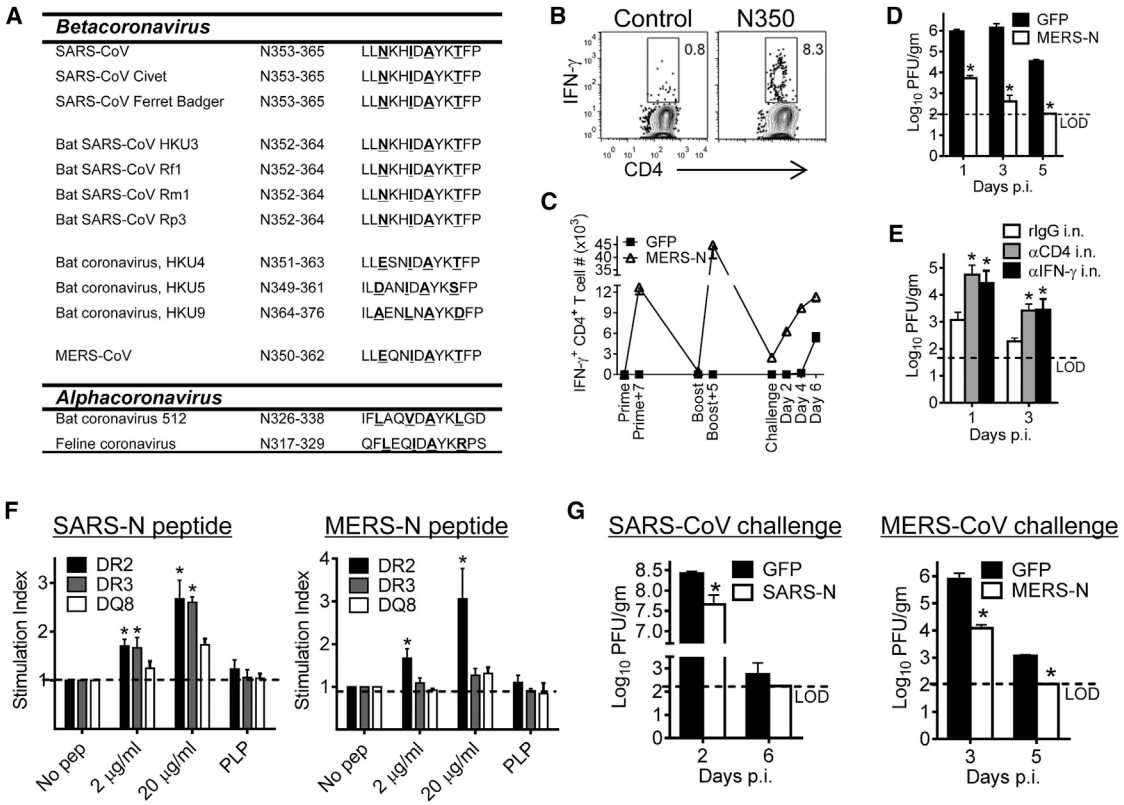

Figure 6. The N-Specific CD4$^+$ T Cell Epitope Is Conserved in MERS-CoV and Is Presented by Human HLA-DR2 and DR3 Molecules

(A) Sequences of SARS-CoV N353 epitope and homologous epitopes in other CoVs are shown. Underlined letters are anchor residues.

(B) Airway-derived cells were prepared from MERS-CoV-infected (1×10^5 PFU) mice at day 6 p.i. and stimulated with peptide. Frequencies of MERS-CoV-specific T cells (determined by IFN-γ intracellular staining) are shown.

(C) Control and VRP-MERS-N-vaccinated mice were infected with MERS-CoV and sacrificed at the indicated time points. Airway cells were stimulated with MERS-N350 peptide for intracellular IFN-γ.

(D and E) Virus titers were obtained from the lungs of VRP-MERS-N-vaccinated mice (D) or vaccinated and antibody i.n.-treated mice (E) at the indicated time points p.i. Titers are expressed as PFU/g tissue. n = 3 mice/group/time point. *$p < 0.05$. Data are representative of two independent experiments.

(F) Human HLA class II transgenic mice were immunized s.c. with N-specific peptides (100 μg) from SARS-CoV (left) or MERS-CoV (right). At 10 days after immunization, lymphocytes prepared from draining lymph nodes were stimulated with N or control proteolipid protein (PLP) peptides in vitro. The results are presented as stimulation indices (cpm of test sample/cpm of the control). *$p < 0.05$. Data are representative of two independent experiments.

(G) HLA-DR2 mice were vaccinated with VRP-SARS-N (left) or VRP-MERS-N (right) i.n. and infected with SARS-CoV or MERS-CoV. Lung virus titers are expressed as PFU/g tissue. n = 3 mice/group/time point. *$p < 0.05$. Data are representative of two independent experiments.

Error bars in (C)–(G) represent SEM. See also Figure S7.

was relatively minor; depletion of airway CD4$^+$ T cells or blockade of airway IFN-γ significantly decreased the rate of virus clearance (Figure 6E).

The region of the N protein encoding SARS-N353 was recognized in some SARS patients (Oh et al., 2011; Peng et al., 2006). To determine whether the SARS-N353 or MERS-N350 epitope was potentially recognized in humans, we immunized mice transgenic for human HLA class II DR2 or DR3 antigen with N peptides and analyzed mice for peptide-specific CD4$^+$ T cell responses. As shown in Figure 6F, SARS-N353 could be presented by both DR2 and DR3, whereas MERS-N350 was successfully presented by DR2. HLA-DR2 and HLA-DR3 transgenic mice are on a C57BL/10 (H-2^b) background. Young SARS-CoV-infected mice on this background do not develop clinical disease (Frieman et al., 2010; Zhao et al., 2011), so we assessed the effect of immunization by measuring the kinetics of virus clearance. Immunization with VRP-SARS-N or VRP-MERS-N enhanced the kinetics of virus clearance from these HLA transgenic mice after challenge with SARS-CoV or MERS-CoV (Figure 6G), indicating that these constructs could be potential vaccine candidates in human populations. No H-2^b-restricted CD8$^+$ T cell epitopes are present in the N protein of either MERS-CoV or SARS-CoV (Zhao et al., 2010, 2014) so that vaccination induced solely a virus-specific CD4$^+$ T cell response.

Cross-reactive CD4$^+$ T Cells Are Protective against SARS-CoV and MERS-CoV

Neutralizing antibodies against SARS-CoV and MERS-CoV are not cross-reactive in humans or mice (Agnihothram et al., 2014) because these antibodies are directed against the highly variable S protein. Having identified closely related analogs to

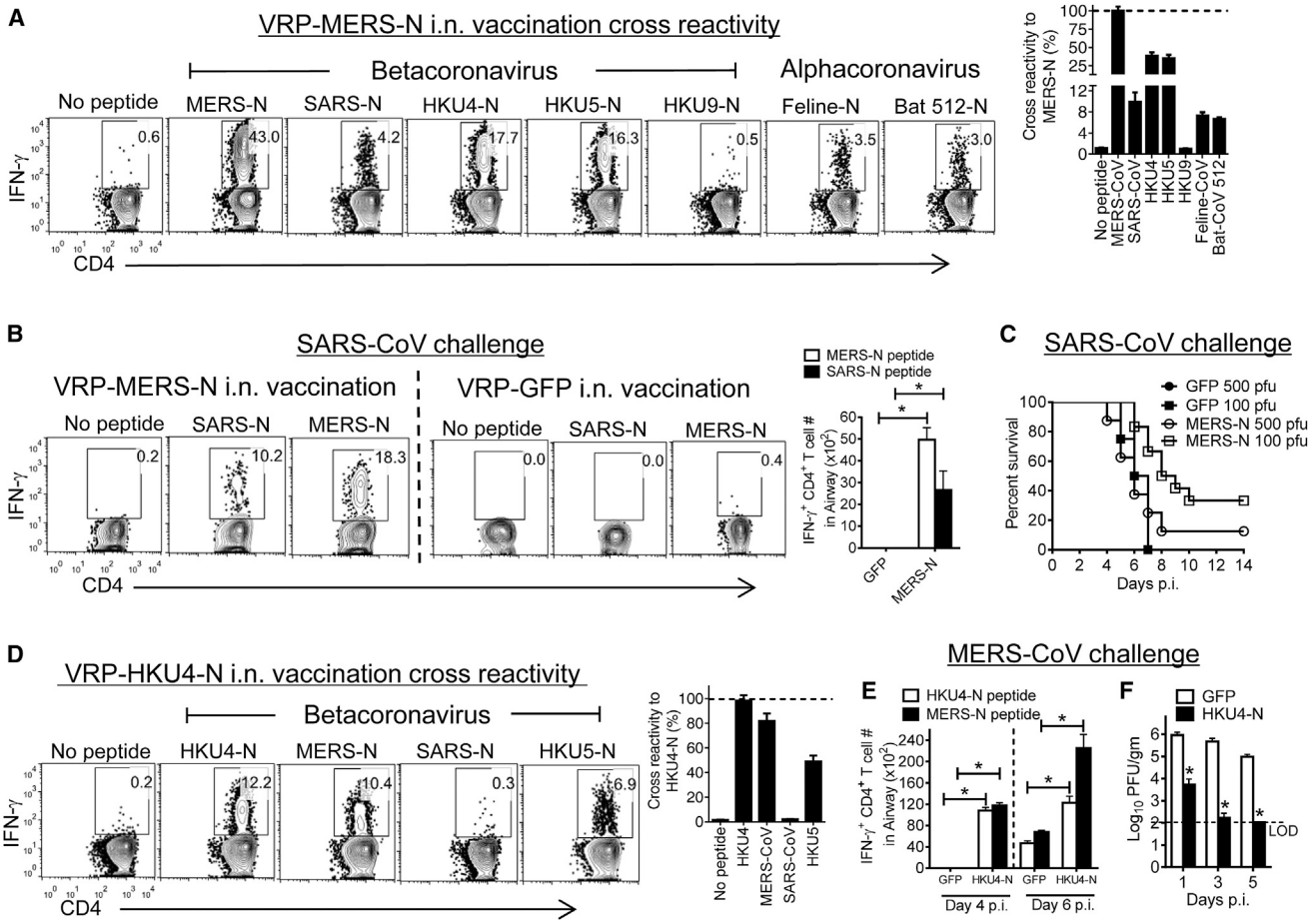

Figure 7. Cross-reactive Memory CD4⁺ T Cells Are Protective against SARS-CoV and MERS-CoV

(A) Airway-derived cells from VRP-MERS-N-vaccinated mice were stimulated with various CoV-specific peptides and assayed for IFN-γ production 5 days after booster. The percentage of cross reactivity between MERS-N peptide and other coronavirus N peptides is shown.

(B) VRP-MERS-N- or VRP-GFP-vaccinated mice were infected with SARS-CoV. Airway-derived cells were stimulated with SARS-N or MERS-N peptides and assayed for IFN-γ production at day 6 p.i. Numbers of CD4⁺ T cells responding to MERS-N350 or SARS-N353 peptides are shown (right). *$p < 0.05$. Data are representative of six independent experiments.

(C) VRP-MERS-N- or VRP-GFP-vaccinated mice were infected with 100 PFU or 500 PFU of SARS-CoV. n = 4, GFP-immunized + 100 PFU SARS-CoV; n = 4, GFP + 500 PFU; n = 12, MERS-N + 100 PFU; n = 8, MERS-N + 500 PFU.

(D) Mice were vaccinated with VRP-HKU4-N. Airway-derived cells were stimulated with CoV-specific peptides and assayed for IFN-γ production. The percentage of cross reactivity between HKU4-N peptide and other coronavirus N peptides is shown.

(E) VRP-HKU4-N- or VRP-GFP-vaccinated mice were infected with MERS-CoV. Airway-derived cells were stimulated with HKU4-N and MERS-N peptides. Numbers of IFN-γ⁺ SARS-N353- and MERS-N350-specific CD4⁺ T cells are shown (right). *$p < 0.05$. Data are representative of three independent experiments.

(F) Virus titers in the lungs are expressed as PFU/g tissue. n = 3 mice/group/time point. *$p < 0.05$. Data are representative of two independent experiments.

Error bars in (A), (B), and (D)–(F) represent SEM.

SARS-N353 in other coronaviruses (Figure 6A), we next asked whether these epitopes induced cross-reactive memory CD4⁺ T cells in the airway. Immunization with VRP-MERS-N induced CD4⁺ T cells that responded to many of the peptides listed in Figure 6A (Figure 7A), whereas VRP-SARS-N immunization induced a small cross-reactive response (<1.0%, data not shown). Next, we assessed whether these VRP-MERS-N-induced cross-reactive memory CD4⁺ T cells were protective against SARS-CoV challenge. After VRP-MERS-N immunization and SARS-CoV challenge, virus-specific airway CD4⁺ T cells were detected after stimulation with either SARS-N353 or MERS-N350 peptides; these cells were not present in infected mice previously immunized with VRP-GFP (Figure 7B). VRP-MERS-N vaccination was partly protective against low-dose SARS-CoV challenge (Figure 7C). This limited protection was most likely because the numbers of cross-reactive N-specific CD4⁺ T cells in the airway were approximately 10-fold lower than detected after VRP-SARS-N immunization (compare Figures 1A and 7B). As we observed strong cross-reactivity between the MERS-CoV and HKU4 and HKU5 epitopes, we examined whether vaccination with VRP-HKU4-N would enhance MERS-CoV clearance. Vaccination with VRP-HKU4-N induced cross-reactive CD4⁺ T cell responses against MERS-CoV N and HKU5 N (Figure 7D). After challenge with MERS-CoV, we detected a robust CD4⁺ T cell

response, with more cells responding to MERS-N350 than to HKU4-N351 (Figure 7E). VRP-HKU4-N vaccination resulted in enhanced MERS-CoV clearance, with kinetics very similar to that observed after VRP-MERS-N vaccination (compare Figures 6D and 7F). Collectively, these results indicate that a conserved epitope recognized by airway memory $CD4^+$ T cells in SARS-CoV- and MERS-CoV-infected mice induced a cross-reactive, protective immune response.

DISCUSSION

No licensed vaccines are available for either SARS-CoV or MERS-CoV, two pathogenic human coronaviruses, and none of the vaccines under development have broad activity. Here we showed that respiratory tract memory $CD4^+$ T cells provided protection against challenge with SARS-CoV and MERS-CoV. Using specific depletion of $CD4^+$ T cells by i.n. administration of antibody, we demonstrated that cells localized to the airway were critical for protection. Airway CoV-specific $CD4^+$ T cells provided the first line of defense against challenge, enhancing the immune response at early and late times after infection. More rapid virus clearance occurred within 1–2 days after challenge, demonstrating the role of airway memory $CD4^+$ T cells in enhancing the innate immune response. At 6–7 days p.i., virus clearance was again accelerated because these cells augmented rDC migration to MLNs and subsequent virus-specific $CD8^+$ T cell priming and mobilization to the infected lungs in a CXCR3-dependent manner. All of these effects were dependent upon airway $CD4^+$ T-cell-derived IFN-γ.

As in humans and other animals infected with coronaviruses, $CD4^+$ T cell epitopes recognized in IAV-infected humans and mice are highly conserved (MacLeod et al., 2010) and elicit protective responses. Protection occurs via IFN-γ expression and enhancement of $CD8^+$ T cell and antibody responses, similar to our findings (McKinstry et al., 2012). In another study, memory $CD4^+$ T cells were identified in the lungs of IAV-infected mice and shown to be lung-resident cells using a parabiosis model. After transfer to naive mice, these lung-derived cells preferentially migrated to the lungs and mediated protection upon subsequent IAV challenge (Teijaro et al., 2011). IAV-specific memory $CD4^+$ T cells also were identified in normal-appearing human lungs (Purwar et al., 2011). Although both of these studies refer to these cells as lung $CD4^+$ Trm cells, our results suggest that this terminology must be used carefully. We showed that there were three populations of cells in the lungs, and at least memory $CD4^+$ T cells in the airways were replenished after a few weeks. Memory $CD4^+$ T cells have specific advantages compared to memory $CD8^+$ T cells because they are longer lived in some settings and are more polyclonal (Lees and Farber, 2010; Stockinger et al., 2006). Consistent with this, we observed that the SARS-N353-specific $CD4^+$ T cell response in the airway demonstrated long-term protection: mice immunized with VRP-SARS-N at 6 weeks of age and challenged 41 weeks after boosting exhibited 30% survival whereas age-matched controls all succumbed to the infection. Further, $CD4^+$ T cell epitopes are less prone to immune escape than are $CD8^+$ T cell epitopes, partly because $CD4^+$ T cells largely function via $CD8^+$ T cell recruitment and other indirect mechanisms whereas virus-specific $CD8^+$ T cells directly target infected cells. Consequently, $CD4^+$ T cell epitope escape has only rarely been described (Harcourt et al., 1998).

We observed that airway, parenchymal, and vascular memory $CD4^+$ T cells differ phenotypically and functionally. First, CD127 and CD27, two memory T cell markers (Mueller et al., 2013), were present at lower levels on airway $CD4^+$ T cells, suggesting that these cells maintained an effector-like phenotype and were delayed in transition to a complete memory phenotype. Second, CD11a, important for retention in tissues, was lower on airway $CD4^+$ T cells, indicating a lack of requirement for tissue adherence and consistent with localization in the airway. Third, airway $CD4^+$ T cells did not express CD103, CD69, and Ly6C, markers for $CD8^+$ Trm cells, unlike parenchymal cells, which resembled $CD8^+$ Trm cells more closely. Finally, airway $CD4^+$ T cells were more multifunctional than cells in the parenchyma and vascular, with a higher percentage of cells producing multiple cytokines and with higher cytokine production on a per cell basis. Airway cells exhibited greater functional avidity than their parenchyma counterparts, arguing that they could rapidly respond at early stages during pathogen challenge while antigen levels were still low.

The N protein is conserved among different coronaviruses and induces cross-reacting antibodies (Woo et al., 2004). However, N-specific sera were non-neutralizing and did not protect against subsequent challenge, as shown in this report and by others (Agnihothram et al., 2014). In contrast, airway memory $CD4^+$ T cells targeting SARS-CoV epitope N353 or its homolog in MERS-CoV and other CoVs induced protective responses. The MERS-CoV and HKU4 N-specific epitopes induced especially strong cross-reactive and protective responses so their inclusion in a vaccine would be expected to increase efficacy against a variety of antigenically variable human coronaviruses. Studies of SARS survivors (Oh et al., 2011; Peng et al., 2006), as well as our analyses of infected DR2 and DR3 Tg mice, indicated that this epitope was also likely to be useful as an immunogen in human populations.

In summary, intranasal vaccine administration generated memory $CD4^+$ T cells that were localized to the airway and were more protective against challenge with pathogenic human coronaviruses than those generated after systemic vaccination. The combination of memory $CD4^+$ T-cell-inducing vaccines with those able to elicit strong neutralizing antibody responses and memory $CD8^+$ T cells would be predicted to result in long-lasting, broad protection against several CoVs. This strategy might also be useful in the context of other pathogenic respiratory viruses.

EXPERIMENTAL PROCEDURES

Mice, Virus, and Cells

Specific-pathogen-free mice were maintained in the Animal Care Facility at the University of Iowa. All protocols were approved by the University of Iowa Institutional Animal Care and Use Committee. The EMC/2012 strain of MERS-CoV (passage 8, designated MERS-CoV) was provided by Drs. Bart Haagmans and Ron Fouchier (Erasmus Medical Center). Mouse-adapted SARS-CoV (MA15) was a kind gift from Dr. Kanta Subbarao (NIH) (Roberts et al., 2007). All work with SARS-CoV and MERS-CoV was conducted in the University of Iowa Biosafety Level 3 (BSL3) Laboratory.

Venezuelan Equine Encephalitis Replicon Particles and Mouse Immunization

Venezuelan equine encephalitis replicon particles (VRPs) expressing the SARS-CoV, MERS-CoV, or HKU4 nucleocapsid proteins (N) were constructed

as previously described (Scobey et al., 2013; Zhao et al., 2014). Mice were primed and boosted (6–7 weeks after priming) with 1 × 10^5 infectious units (IU) of VRP-SARS-N, VRP-SARS-S, or VRP-GFP in the left footpad in 20 μL PBS or intranasally (i.n.) in 50 μL PBS after light anesthesia with isoflurane. Mice were challenged with SARS-CoV or MERS-CoV 4–6 weeks after boosting.

Transduction and Infection of Mice

Recombinant adenoviral vectors expressing-hDPP4 (Ad5-DPP4) were prepared and used as previously described (Zhao et al., 2014). Mice were infected with indicated doses of MERS-CoV or SARS-CoV in 50 μL DMEM.

Preparation of Cells from Bronchoalveolar Lavage Fluids, Lungs, and MLNs

Mice were sacrificed at the indicated time points. BALF was acquired by inflating lungs with 1 mL complete RPMI 1640 medium via cannulation of the trachea followed by lavaging four times. Cells in the bronchoalveolar lavage fluid (BALF) were collected by centrifugation. Cells were prepared from the lungs and MLNs as previously described (Zhao et al., 2011).

Simultaneous Intranasal and Intravascular Antibody Labeling

Mice were lightly anesthetized with isoflurane and treated i.n. with 0.25 μg fluorochrome-conjugated CD45 antibody in 100 μL PBS. After 2 min, mice were injected i.v. with 0.5 μg of fluorochrome-conjugated CD90.2 antibody for an additional 3 min prior to euthanasia as previously described (Anderson et al., 2012). Mice were perfused and cells from the airway and lungs were prepared.

Antibody and Cytokine Treatment

For systemic depletion of $CD4^+$ or $CD8^+$ T cells, mice were injected intraperitoneally (i.p.) with 1 mg anti-CD4 antibody (clone GK1.5) or 500 μg anti-CD8 antibody (clone 2.43), respectively, at days −2 and 0 p.i. For airway depletion of $CD4^+$ T cells, mice were lightly anesthetized with isoflurane and treated with 10 μg anti-CD4 antibody i.n. in 75 μL PBS at day −1 p.i. For systemic neutralization/blockade of IFN-γ and IL-10, mice were injected i.p. with 500 μg of anti-IFN-γ antibody (clone XMG1.2) or anti-IL-10 receptor antibody (clone 1B1.3A) at day −2, 0, 2, 4, 6, and 8 p.i. For airway neutralization of IFN-γ, mice were treated i.n. with 10 μg of anti-IFN-γ antibody (clone XMG1.2) at day −2, 0, 2, 4, 6, and 8 p.i. CXCR3 was blocked with i.p. injection of 500 μg of anti-CXCR3 antibody (clone CXCR3-173) at days 3 and 5 p.i. Control mice received equivalent doses of rat or Armenian Hamster IgG in each experiment. All antibodies were acquired from Bio X cell. For cytokine treatment, mice were treated with 200 ng rIFN-γ or rTNF (R&D Systems) intranasally in 50 μL PBS 12 hr before infection.

Statistical Analysis

A Student's t test was used to analyze differences in mean values between groups. All results are expressed as means ± SEM. p values of < 0.05 were considered statistically significant.

SUPPLEMENTAL INFORMATION

Supplemental Information includes seven figures and Supplemental Experimental Procedures and can be found with this article online at http://dx.doi.org/10.1016/j.immuni.2016.05.006.

AUTHOR CONTRIBUTIONS

Jincun Zhao, Jingxian Zhao, and S.P. designed and coordinated the study. Jincun Zhao, Jingxian Zhao, A.K.M., R.C., C.F., and D.K.M. performed the experiments. S.A. and R.S.B. provided the VRP platform. C.S.D. provided the HLA class II transgenic mice. Jincun Zhao and S.P. wrote the manuscript. All authors contributed to the interpretation and conclusions presented.

ACKNOWLEDGMENTS

We thank Drs. John Harty and Kevin Legge for critical review of the manuscript. This research was supported in part by grants from the NIH (RO1 AI091322 and PO1 AI060699 to S.P. and U19 AI100625 R.S.B.), the Thousand Talents Plan Award of China 2015, and the Municipal Healthcare Joint-Innovation Major Project of Guangzhou (Jincun Zhao).

Received: November 19, 2015
Revised: February 14, 2016
Accepted: March 8, 2016
Published: June 7, 2016

REFERENCES

Agnihothram, S., Gopal, R., Yount, B.L., Jr., Donaldson, E.F., Menachery, V.D., Graham, R.L., Scobey, T.D., Gralinski, L.E., Denison, M.R., Zambon, M., and Baric, R.S. (2014). Evaluation of serologic and antigenic relationships between middle eastern respiratory syndrome coronavirus and other coronaviruses to develop vaccine platforms for the rapid response to emerging coronaviruses. J. Infect. Dis. *209*, 995–1006.

Anderson, K.G., Sung, H., Skon, C.N., Lefrancois, L., Deisinger, A., Vezys, V., and Masopust, D. (2012). Cutting edge: intravascular staining redefines lung CD8 T cell responses. J. Immunol. *189*, 2702–2706.

Bolles, M., Deming, D., Long, K., Agnihothram, S., Whitmore, A., Ferris, M., Funkhouser, W., Gralinski, L., Totura, A., Heise, M., and Baric, R.S. (2011). A double-inactivated severe acute respiratory syndrome coronavirus vaccine provides incomplete protection in mice and induces increased eosinophilic proinflammatory pulmonary response upon challenge. J. Virol. *85*, 12201–12215.

Channappanavar, R., Zhao, J., and Perlman, S. (2014). T cell-mediated immune response to respiratory coronaviruses. Immunol. Res. *59*, 118–128.

Chinese SARS Molecular Epidemiology Consortium (2004). Molecular evolution of the SARS coronavirus during the course of the SARS epidemic in China. Science *303*, 1666–1669.

Frieman, M.B., Chen, J., Morrison, T.E., Whitmore, A., Funkhouser, W., Ward, J.M., Lamirande, E.W., Roberts, A., Heise, M., Subbarao, K., and Baric, R.S. (2010). SARS-CoV pathogenesis is regulated by a STAT1 dependent but a type I, II and III interferon receptor independent mechanism. PLoS Pathog. *6*, e1000849.

Ge, X.Y., Li, J.L., Yang, X.L., Chmura, A.A., Zhu, G., Epstein, J.H., Mazet, J.K., Hu, B., Zhang, W., Peng, C., et al. (2013). Isolation and characterization of a bat SARS-like coronavirus that uses the ACE2 receptor. Nature *503*, 535–538.

Harcourt, G.C., Garrard, S., Davenport, M.P., Edwards, A., and Phillips, R.E. (1998). HIV-1 variation diminishes CD4 T lymphocyte recognition. J. Exp. Med. *188*, 1785–1793.

Hufford, M.M., Kim, T.S., Sun, J., and Braciale, T.J. (2011). Antiviral CD8+ T cell effector activities in situ are regulated by target cell type. J. Exp. Med. *208*, 167–180.

Iwata-Yoshikawa, N., Uda, A., Suzuki, T., Tsunetsugu-Yokota, Y., Sato, Y., Morikawa, S., Tashiro, M., Sata, T., Hasegawa, H., and Nagata, N. (2014). Effects of Toll-like receptor stimulation on eosinophilic infiltration in lungs of BALB/c mice immunized with UV-inactivated severe acute respiratory syndrome-related coronavirus vaccine. J. Virol. *88*, 8597–8614.

Lees, J.R., and Farber, D.L. (2010). Generation, persistence and plasticity of CD4 T-cell memories. Immunology *130*, 463–470.

Li, W., Shi, Z., Yu, M., Ren, W., Smith, C., Epstein, J.H., Wang, H., Crameri, G., Hu, Z., Zhang, H., et al. (2005). Bats are natural reservoirs of SARS-like coronaviruses. Science *310*, 676–679.

Ma, C., Wang, L., Tao, X., Zhang, N., Yang, Y., Tseng, C.T., Li, F., Zhou, Y., Jiang, S., and Du, L. (2014). Searching for an ideal vaccine candidate among different MERS coronavirus receptor-binding fragments–the importance of immunofocusing in subunit vaccine design. Vaccine *32*, 6170–6176.

MacLeod, M.K., Kappler, J.W., and Marrack, P. (2010). Memory CD4 T cells: generation, reactivation and re-assignment. Immunology *130*, 10–15.

Masopust, D., and Picker, L.J. (2012). Hidden memories: frontline memory T cells and early pathogen interception. J. Immunol. *188*, 5811–5817.

McKinstry, K.K., Strutt, T.M., Kuang, Y., Brown, D.M., Sell, S., Dutton, R.W., and Swain, S.L. (2012). Memory CD4+ T cells protect against influenza through multiple synergizing mechanisms. J. Clin. Invest. *122*, 2847–2856.

Moran, T.P., Collier, M., McKinnon, K.P., Davis, N.L., Johnston, R.E., and Serody, J.S. (2005). A novel viral system for generating antigen-specific T cells. J. Immunol. *175*, 3431–3438.

Mueller, S.N., Gebhardt, T., Carbone, F.R., and Heath, W.R. (2013). Memory T cell subsets, migration patterns, and tissue residence. Annu. Rev. Immunol. *31*, 137–161.

Oh, H.L., Chia, A., Chang, C.X., Leong, H.N., Ling, K.L., Grotenbreg, G.M., Gehring, A.J., Tan, Y.J., and Bertoletti, A. (2011). Engineering T cells specific for a dominant severe acute respiratory syndrome coronavirus CD8 T cell epitope. J. Virol. *85*, 10464–10471.

Peiris, J.S., Guan, Y., and Yuen, K.Y. (2004). Severe acute respiratory syndrome. Nat. Med. *10* (12, Suppl), S88–S97.

Peng, H., Yang, L.T., Wang, L.Y., Li, J., Huang, J., Lu, Z.Q., Koup, R.A., Bailer, R.T., and Wu, C.Y. (2006). Long-lived memory T lymphocyte responses against SARS coronavirus nucleocapsid protein in SARS-recovered patients. Virology *351*, 466–475.

Purwar, R., Campbell, J., Murphy, G., Richards, W.G., Clark, R.A., and Kupper, T.S. (2011). Resident memory T cells (T(RM)) are abundant in human lung: diversity, function, and antigen specificity. PLoS ONE *6*, e16245.

Roberts, A., Deming, D., Paddock, C.D., Cheng, A., Yount, B., Vogel, L., Herman, B.D., Sheahan, T., Heise, M., Genrich, G.L., et al. (2007). A mouse-adapted SARS-coronavirus causes disease and mortality in BALB/c mice. PLoS Pathog. *3*, e5.

Scobey, T., Yount, B.L., Sims, A.C., Donaldson, E.F., Agnihothram, S.S., Menachery, V.D., Graham, R.L., Swanstrom, J., Bove, P.F., Kim, J.D., et al. (2013). Reverse genetics with a full-length infectious cDNA of the Middle East respiratory syndrome coronavirus. Proc. Natl. Acad. Sci. USA *110*, 16157–16162.

Slütter, B., Pewe, L.L., Kaech, S.M., and Harty, J.T. (2013). Lung airway-surveilling CXCR3(hi) memory CD8(+) T cells are critical for protection against influenza A virus. Immunity *39*, 939–948.

Stockinger, B., Bourgeois, C., and Kassiotis, G. (2006). CD4+ memory T cells: functional differentiation and homeostasis. Immunol. Rev. *211*, 39–48.

Sui, J., Deming, M., Rockx, B., Liddington, R.C., Zhu, Q.K., Baric, R.S., and Marasco, W.A. (2014). Effects of human anti-spike protein receptor binding domain antibodies on severe acute respiratory syndrome coronavirus neutralization escape and fitness. J. Virol. *88*, 13769–13780.

Sun, J., Madan, R., Karp, C.L., and Braciale, T.J. (2009). Effector T cells control lung inflammation during acute influenza virus infection by producing IL-10. Nat. Med. *15*, 277–284.

Swain, S.L., McKinstry, K.K., and Strutt, T.M. (2012). Expanding roles for $CD4^+$ T cells in immunity to viruses. Nat. Rev. Immunol. *12*, 136–148.

Tang, F., Quan, Y., Xin, Z.T., Wrammert, J., Ma, M.J., Lv, H., Wang, T.B., Yang, H., Richardus, J.H., Liu, W., and Cao, W.C. (2011). Lack of peripheral memory B cell responses in recovered patients with severe acute respiratory syndrome: a six-year follow-up study. J. Immunol. *186*, 7264–7268.

Teijaro, J.R., Turner, D., Pham, Q., Wherry, E.J., Lefrançois, L., and Farber, D.L. (2011). Cutting edge: Tissue-retentive lung memory CD4 T cells mediate optimal protection to respiratory virus infection. J. Immunol. *187*, 5510–5514.

Tonkin, D.R., Whitmore, A., Johnston, R.E., and Barro, M. (2012). Infected dendritic cells are sufficient to mediate the adjuvant activity generated by Venezuelan equine encephalitis virus replicon particles. Vaccine *30*, 4532–4542.

Trandem, K., Zhao, J., Fleming, E., and Perlman, S. (2011). Highly activated cytotoxic CD8 T cells express protective IL-10 at the peak of coronavirus-induced encephalitis. J. Immunol. *186*, 3642–3652.

Turner, D.L., and Farber, D.L. (2014). Mucosal resident memory CD4 T cells in protection and immunopathology. Front. Immunol. *5*, 331.

Wang, X., Liao, Y., Yap, P.L., Png, K.J., Tam, J.P., and Liu, D.X. (2009). Inhibition of protein kinase R activation and upregulation of GADD34 expression play a synergistic role in facilitating coronavirus replication by maintaining de novo protein synthesis in virus-infected cells. J. Virol. *83*, 12462–12472.

Wilkinson, T.M., Li, C.K., Chui, C.S., Huang, A.K., Perkins, M., Liebner, J.C., Lambkin-Williams, R., Gilbert, A., Oxford, J., Nicholas, B., et al. (2012). Preexisting influenza-specific CD4+ T cells correlate with disease protection against influenza challenge in humans. Nat. Med. *18*, 274–280.

Woo, P.C., Lau, S.K., Wong, B.H., Chan, K.H., Hui, W.T., Kwan, G.S., Peiris, J.S., Couch, R.B., and Yuen, K.Y. (2004). False-positive results in a recombinant severe acute respiratory syndrome-associated coronavirus (SARS-CoV) nucleocapsid enzyme-linked immunosorbent assay due to HCoV-OC43 and HCoV-229E rectified by Western blotting with recombinant SARS-CoV spike polypeptide. J. Clin. Microbiol. *42*, 5885–5888.

Zhao, J., Zhao, J., and Perlman, S. (2010). T cell responses are required for protection from clinical disease and for virus clearance in severe acute respiratory syndrome coronavirus-infected mice. J. Virol. *84*, 9318–9325.

Zhao, J., Zhao, J., Legge, K., and Perlman, S. (2011). Age-related increases in PGD(2) expression impair respiratory DC migration, resulting in diminished T cell responses upon respiratory virus infection in mice. J. Clin. Invest. *121*, 4921–4930.

Zhao, L., Jha, B.K., Wu, A., Elliott, R., Ziebuhr, J., Gorbalenya, A.E., Silverman, R.H., and Weiss, S.R. (2012). Antagonism of the interferon-induced OAS-RNase L pathway by murine coronavirus ns2 protein is required for virus replication and liver pathology. Cell Host Microbe *11*, 607–616.

Zhao, J., Li, K., Wohlford-Lenane, C., Agnihothram, S.S., Fett, C., Zhao, J., Gale, M.J., Jr., Baric, R.S., Enjuanes, L., Gallagher, T., et al. (2014). Rapid generation of a mouse model for Middle East respiratory syndrome. Proc. Natl. Acad. Sci. USA *111*, 4970–4975.

Immunity, Volume *44*

Supplemental Information

Airway Memory CD4^{+} T Cells Mediate Protective Immunity against Emerging Respiratory Coronaviruses

Jincun Zhao, Jingxian Zhao, Ashutosh K. Mangalam, Rudragouda Channappanavar, Craig Fett, David K. Meyerholz, Sudhakar Agnihothram, Ralph S. Baric, Chella S. David, and Stanley Perlman

Supplemental Figure 1

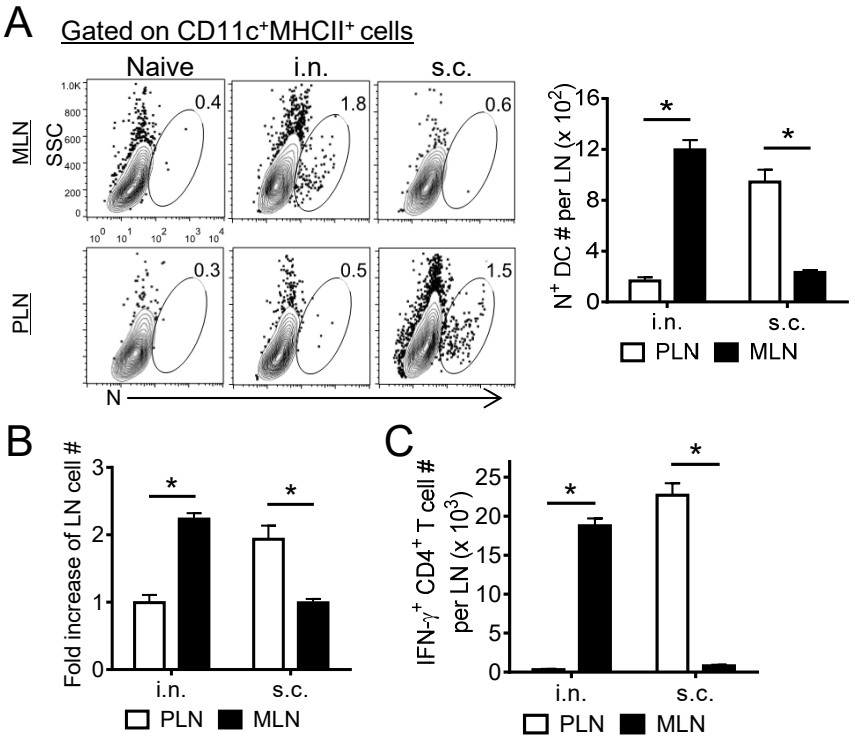

Figure S1 related to Figure 1. VRP-SARS-N infected DCs presented antigen in the regional DLNs. (**A**) To determine DC migration from vaccinated lung or footpad to DLNs, mice were vaccinated with VRP-SARS-N i.n. or s.c. After 18 hours, single cell suspensions were prepared from MLNs or PLNs. Cells were labeled with 1:1000 diluted anti-SARS-N mouse serum, followed by Alexa488-goat anti mouse IgG. The numbers represent the percentage of N^+ DC population (left) and total N^+ DC numbers per LN (right). (**B**) Fold increase of cell numbers in the DLNs at 18 hours post vaccination. (**C**) Cells from DLN were prepared at day 5 post vaccination and stimulated with N353 peptide in the presence of BFA. Cells were then stained for intracellular IFN-γ. IFN-γ^+ SARS-N353-specific $CD4^+$ T cell numbers per LN are shown. *n*= 3 mice/group. **P* values of <0.05. Error bars represent SEM. Data are representative of 2 independent experiments.

Supplemental Figure 2

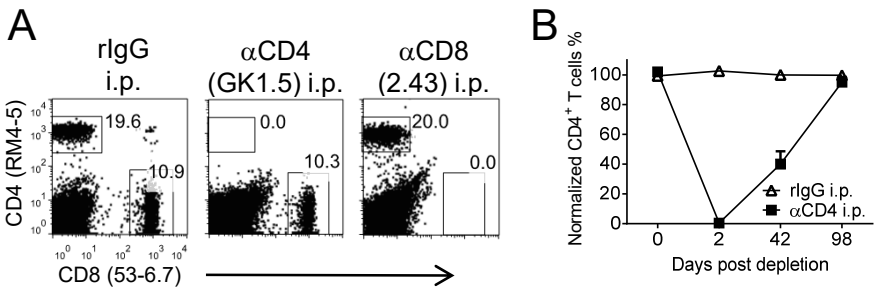

Figure S2 related to Figures 1 and 5. T cell depletion. (**A, B**) For systemic depletion of $CD4^+$ or $CD8^+$ T cells, mice were injected intraperitoneally (i.p.) with 1 mg anti-CD4 antibody (GK1.5) or 500 μg anti-CD8 antibody (2.43) at day -2 and day 0, respectively. Whole lungs were harvested at day 1 (**A**), or blood was harvested at indicated time points (**B**). Error bars represent SEM.

Supplemental Figure 3

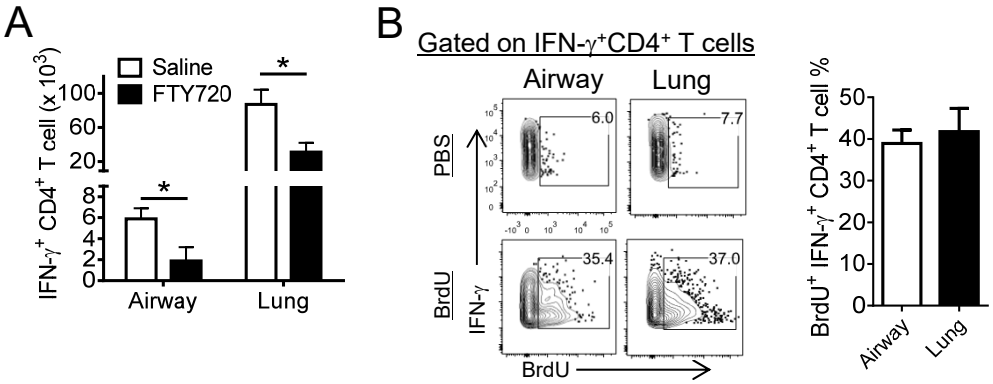

Figure S3 related to Figure 2. Recruitment from lymphoid organs and *in situ* proliferation contribute to protective CD4⁺ T responses in the respiratory tract. VRP-SARS-N i.n. vaccinated mice were treated with FTY720 (4 mg/kg) in saline i.p. daily starting one day prior to infection with 500 PFU SARS-CoV. (**A**) Cells from airways and lungs were stimulated with SARS-N353 peptide day 4 p.i. Numbers of IFN-γ⁺ CD4⁺ T cells are shown. (**B**) 1 mg BrdU in 100 μl PBS was delivered to FTY720 treated mice i.n. at day 4 p.i. After 4 hours, mice were sacrificed and cells from airways and lungs were stimulated with SARS-N353 peptide. Frequencies of BrdU⁺IFN-γ⁺ CD4⁺ T cells are shown. *n*= 3 mice/group. Error bars represent SEM. Data are representative of 3 independent experiments.

Supplemental Figure 4

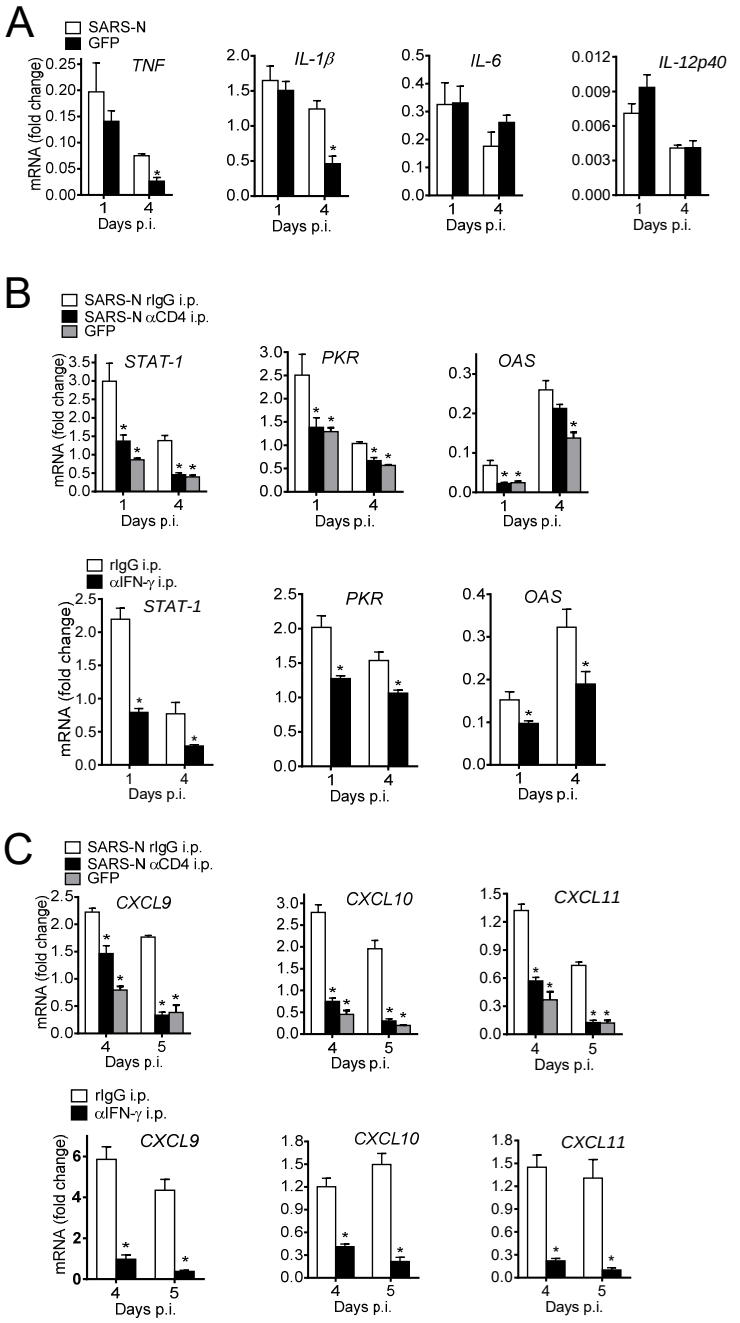

Figure S4 related to Figures 3 and 5. Pro-inflammatory cytokine mRNA levels. (**A, B, C**) Vaccinated mice were treated with anti-CD4 antibody, IFN-γ neutralizing antibody, or control antibody i.p. before SARS-CoV infection. Lungs were harvested at the indicated time points p.i. mRNA levels in the lungs were measured. *n*= 3-6 mice/group/time point. **P*<0.05. Error bars represent SEM. Data are representative of 2 independent experiments.

Supplemental Figure 5

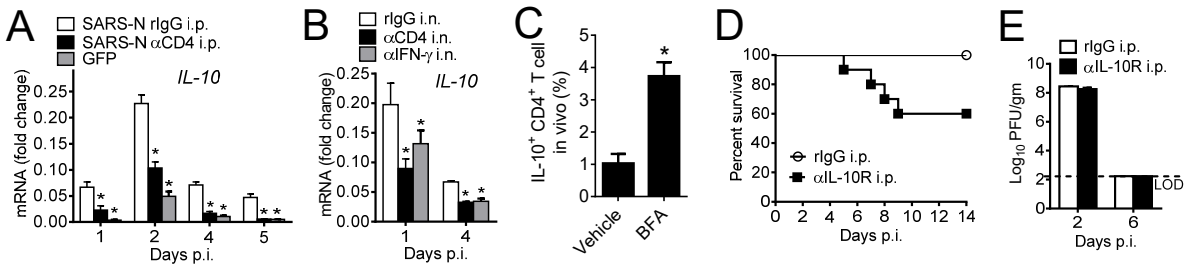

Figure S5 related to Figure 2. IL-10R blockade increased mortality in SARS-CoV infected mice. (**A, B**) VRP-SARS-N vaccinated mice were treated with anti-CD4 antibody (GK1.5) or rIgG i.p. (**A**) or anti-CD4 antibody (GK1.5) or anti-IFN-γ (XMG1.2) or rIgG i.n. (**B**). Mice were then infected with 500 PFU SARS-CoV. Lungs were harvested at indicated time points and IL-10 mRNA levels measured. *n*= 3-6 mice/group/time point. **P* values of <0.05. Error bars represent SEM. Data are representative of 2 independent experiments. (**C**) For *in vivo* ICS, VRP-SARS-N vaccinated mice were treated with BFA i.n. or vehicle at day 6 p.i. After 6 hours, lung-derived $CD4^+$ T cells were analyzed for IL-10 expression. $IL\text{-}10^+$ SARS-N353-specific $CD4^+$ T frequency is shown. Error bars represent SEM. (**D**) VRP-SARS-N vaccinated mice were treated i.p. with anti-IL-10R antibody (clone 1B1.3A), or equivalent doses of rIgG. Mice were infected with SARS-CoV. *n*= 5, rIgG i.p.; *n*= 10, αIL-10R i.p. (**E**) To obtain virus titers, mice were treated with antibodies as in (**D**). Titers are expressed as PFU/g tissue. n= 3 mice/group/time point. Error bars represent SEM. Data are representative of 2 independent experiments.

Supplemental Figure 6

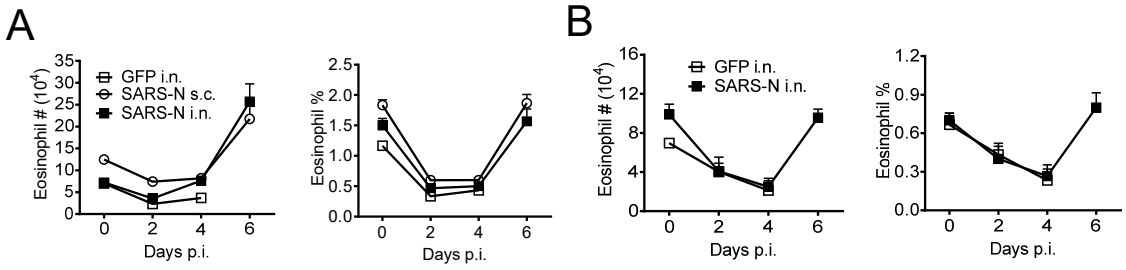

Figure S6 related to Figure 1. Eosinophils in SARS-CoV infected lungs. 6 week-old (**A**) and 12 month-old (**B**) BALB/c mice were vaccinated with VRP-SARS-N or VRP GFP. Mice were infected with 500 PFU (**A**) or 100 PFU (**B**) SARS-CoV. At indicated time p.i., cells from lungs were prepared and stained for eosinophils ($CD45^+CD11c^+SiglecF^+$). Most of the mice in the GFP group died by day 6. Data from days 0-4 are shown. *n*= 3-4 mice/group/time point. Error bars represent SEM. Data are representative of 2 independent experiments.

Supplemental Figure 7

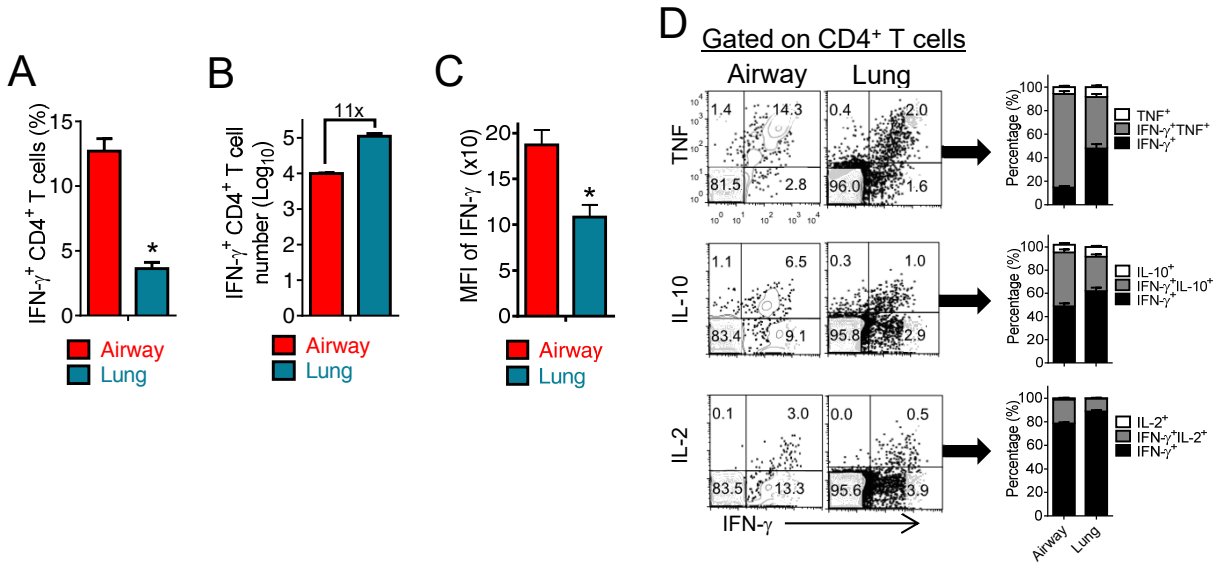

Figure S7 related to Figure 6. Airway-derived N350-specific CD4⁺ T cells are superior effector cells in MERS-CoV infected mice. Vaccinated mice were infected with MERS-CoV at the indicated times. Cells from airway and lung were stimulated with MERS-N350 peptide. Frequency (**A**), numbers (**B**) and mean fluorescence intensities (MFI) of IFN-γ (**C**) of IFN-γ⁺ CD4⁺ T cells or cells expressing IFN-γ and TNF, IL-10 or IL-2 (**D**) are shown. *n*= 3-4 mice/group. Error bars represent SEM. Data are representative of 3 independent experiments.

SUPPLEMENTAL EXPERIMENTAL PROCEDURES

Mice, virus and cells. Specific pathogen-free 6 week and 12 month old BALB/c mice were purchased from the National Cancer Institute and Charles River Laboratories International. HLA-DR2 (DRB1*1501), HLA-DR3 (DRB1*0301) and HLA-DQ8 (DQA1*0301/DQB*0302) transgenic mice were produced as previously described(Cheng et al., 1996; Koehm et al., 2007; Kong et al., 1996). Mice were maintained in the Animal Care Facility at the University of Iowa. All protocols were approved by the University of Iowa Institutional Animal Care and Use Committee. The EMC/2012 strain of MERS-CoV (passage 8, designated MERS-CoV) was provided by Drs. Bart Haagmans and Ron Fouchier *(*Erasmus Medical Center*)*. Mouse-adapted SARS-CoV (MA15) was a kind gift from Dr. Kanta Subbarao (N.I.H., Bethesda, Maryland)(Roberts et al., 2007). SARS-CoV and MERS-CoV were passaged once on Vero E6 or Vero 81 cells and titered on the same cell line. A20 cells were used as antigen presenting cells. All work with SARS-CoV and MERS-CoV was conducted in the University of Iowa Biosafety Level 3 (BSL3) Laboratory.

Venezuelan Equine Encephalitis Replicon particles (VRPs), recombinant vaccinia virus and mouse immunization. VRPs expressing the SARS-CoV, MERS-CoV or HKU4 nucleocapsid proteins (N) were constructed as previously described(Scobey et al., 2013; Zhao et al., 2014). Mice were primed and boosted (6-7 weeks after priming) with $1x10^5$ Infectious Units (IU) of VRP-SARS-N, VRP-SARS-S or VRP-GFP in the left footpad in 20 μl PBS or intranasally (i.n.) in 50 μl PBS after light anesthesia with isoflurane. Recombinant vaccinia virus expressing SARS-CoV N protein was generated as previously described(Castro and Perlman, 1995). Mice were immunized intravenously (i.v.) with $1x10^6$ PFU rVV-N or irrelevant rVV in 200 μl PBS or i.n. in 50 μl PBS after light anesthesia with isoflurane**.** For sera transfer, sera were

obtained from vaccinated mice 2-4 weeks after boosting. Mice were challenged with SARS-CoV or MERS-CoV 4-6 weeks post boosting.

Virus titers. Virus was titered on Vero E6 cells or Vero 81 cells as previously described (Zhao et al., 2014).

Histology and immunohistochemistry. Lungs were removed, fixed in zinc formalin, and paraffin embedded. Sections were stained with hematoxylin and eosin for histological analysis.

Flow cytometry. The following anti-mouse monoclonal antibodies were used: CD4 (RM4-5; GK1.5); CD8α (53-6.7; 2.43); CD90.2 (53-2.1); IFN-γ (XMG1.2); TNF (MP6-XT22); IL-2 (JEH6-5H4); IL-10 (JES-2A5); CD16/32 (2.4G2); CD11a (M17/4); CD27 (LG.7F9); CD44 (IM7); CD49d (R1-2); CD69 (H1.2F3); CD103 (2E7); CD127 (eBioSB/199); Ly6C (AL-21); CXCR3 (CXCR3-173); CCR4 (2G12); CCR5 (HM-CCR5); CD11c (HL3); Siglec F (E50-2440); I-A/E (M5/114.15.2); CCR7 (4B12); CD45 (30-F11); CD40 (HM40-3); CD80 (16-10A1); CD86 (GL1); T-bet (eBio4B10); CD107a (eBio1D4B); CD107b (ABL-93); Granzyme B (16G6), all antibodies were from BD Bioscience, eBioscience or Biolegend.

For surface staining, 10^6 cells were blocked with 1 μg anti-CD16/32 antibody and 1% rat serum, and stained with the indicated antibodies at 4^{o}C, except for those stained with CCR7, which were stained at 37^{o}C.

For *in vitro* intracellular cytokine/protein staining, 1×10^6 cells/well were cultured in 96-well dishes at 37^{o}C for 5-6 hours in the presence of 2.5-10 μM peptide (BioSynthesis Inc., Lewisville, TX), brefeldin A (BFA, BD Biosciences) and antigen presenting cells (A20 cells). Cells were then labeled for cell surface markers, fixed/permeabilized with Cytofix/Cytoperm Solution (BD Biosciences) and labeled with anti-intracellular cytokine/protein antibodies.

To assess functional avidity, cells were stimulated with graded doses of the relevant peptide pulsed onto A20 cells and examined for IFN-γ production. The frequency of $CD4^+$ T cells producing IFN-γ at each concentration of peptide was measured and expressed as a percentage of the maximum response detected. Data were fit to sigmoidal dose–response curves and used to calculate the amount of peptide needed to reach a half-maximum response (EC_{50}).

For *in vivo* intracellular cytokine staining, infected mice were treated with 50 μg BFA (Sigma-Aldrich) or vehicle (DMSO) i.n**.** 6 h later, lung-derived lymphocytes were analyzed directly *ex vivo* for IFN-γ or IL-10 expression as described previously(Hufford et al., 2011).

For N^+ rDC staining, cells from MLNs were labeled for cell surface markers, fixed/permeabilized with Cytofix/Cytoperm Solution (BD Biosciences) and labeled with 1:1000 diluted anti-N serum, followed by A488-Goat anti mouse IgG.

For MHC class II tetramer staining, cells were stained with 8 μg/ml APC-conjugated $I\text{-}A^b$ /N353 tetramers (obtained from the National Institutes of Health/National Institute of Allergy and Infection Diseases MHC Tetramer Core Facility, Atlanta, GA) in complete RPMI 1640 media for 1 h at 37°C. Cells were then incubated with surface and intracellular markers.

All flow cytometry data were acquired on a BD FACSCalibur or BD FACSVerse and analyzed using FlowJo software (Tree Star, Inc.).

In situ CFSE staining. CFSE (Molecular Probes) (8 mM) was administered i.n. (50 μl/mouse) 6 hours before infection(Legge and Braciale, 2003).

In vivo cytotoxicity assay. *In vivo* cytotoxicity assays in the lungs were performed and analyzed on day 6 p.i., as previously described(Barber et al., 2003; Zhao et al., 2009).

Cytokine and chemokine RNA levels in infected lungs using qRT-PCR. RNA was extracted from infected lungs using Trizol (Invitrogen), and used as a template for cDNA synthesis (Invitrogen). qRT-PCR was performed using a previously described set of primers (Zhao et al., 2011).

Peptide immunization and T cell proliferation assay. Mice were immunized subcutaneously with N peptides (100 μg) emulsified in CFA and sacrificed 10 days later; draining lymph nodes were removed and stimulated with peptides *in vitro*. The results are presented as stimulation indices (cpm of test sample/cpm of the control).

FTY720 and BrdU treatment. Vaccinated mice were treated with FTY720 (4 mg/kg) (Cayman, Ann Arbor, MI) in saline i.p. daily starting one day prior to SARS-CoV infection. 1 mg BrdU (BD) in 100 μl PBS was delivered i.n. to FTY720-treated mice at day 4 p.i., 4 hours before sacrifice. Intracellular detection of BrdU was performed using reagents and protocols provided by the manufacturer (BD).

SUPPLEMENTAL REFERENCES

Barber, D.L., Wherry, E.J., and Ahmed, R. (2003). Cutting edge: rapid in vivo killing by memory CD8 T cells. J Immunol *171*, 27-31.

Castro, R.F., and Perlman, S. (1995). CD8+ T-cell epitopes within the surface glycoprotein of a neurotropic coronavirus and correlation with pathogenicity. J Virol *69*, 8127-8131.

Cheng, S., Baisch, J., Krco, C., Savarirayan, S., Hanson, J., Hodgson, K., Smart, M., and David, C. (1996). Expression and function of HLA-DQ8 (DQA1*0301/DQB1*0302) genes in transgenic mice. Eur J Immunogenet *23*, 15-20.

Hufford, M.M., Kim, T.S., Sun, J., and Braciale, T.J. (2011). Antiviral CD8+ T cell effector activities in situ are regulated by target cell type. J Exp Med *208*, 167-180.

Koehm, S., Slavin, R.G., Hutcheson, P.S., Trejo, T., David, C.S., and Bellone, C.J. (2007). HLA-DRB1 alleles control allergic bronchopulmonary aspergillosis-like pulmonary responses in humanized transgenic mice. J Allergy Clin Immunol *120*, 570-577.

Kong, Y.C., Lomo, L.C., Motte, R.W., Giraldo, A.A., Baisch, J., Strauss, G., Hammerling, G.J., and David, C.S. (1996). HLA-DRB1 polymorphism determines susceptibility to autoimmune thyroiditis in transgenic mice: definitive association with HLA-DRB1*0301 (DR3) gene. J Exp Med *184*, 1167-1172.

Legge, K.L., and Braciale, T.J. (2003). Accelerated migration of respiratory dendritic cells to the regional lymph nodes is limited to the early phase of pulmonary infection. Immunity *18*, 265-277.

Roberts, A., Deming, D., Paddock, C.D., Cheng, A., Yount, B., Vogel, L., Herman, B.D., Sheahan, T., Heise, M., Genrich, G.L.*, et al.* (2007). A mouse-adapted SARS-coronavirus causes disease and mortality in BALB/c mice. PLoS Pathog *3*, e5.

Scobey, T., Yount, B.L., Sims, A.C., Donaldson, E.F., Agnihothram, S.S., Menachery, V.D., Graham, R.L., Swanstrom, J., Bove, P.F., Kim, J.D.*, et al.* (2013). Reverse genetics with a full-length infectious cDNA of the Middle East respiratory syndrome coronavirus. Proc Natl Acad Sci *110*, 16157-16162.

Zhao, J., Li, K., Wohlford-Lenane, C., Agnihothram, S.S., Fett, C., Gale, M.J., Jr., Baric, R.S., Enjuanes, L., Gallagher, T., McCray, P.B., Jr., and Perlman, S. (2014). Rapid generation of a mouse model for Middle East respiratory syndrome. Proc Natl Acad Sci *111*, 4970-4975.

Zhao, J., Zhao, J., Legge, K., and Perlman, S. (2011). Age-related increases in PGD(2) expression impair respiratory DC migration, resulting in diminished T cell responses upon respiratory virus infection in mice. J Clin Invest *121*, 4921-4930.

Zhao, J., Zhao, J., Van Rooijen, N., and Perlman, S. (2009). Evasion by stealth: inefficient immune activation underlies poor T cell response and severe disease in SARS-CoV-infected mice. PLoS Pathog *5*, e1000636.